Impact of the day/night cycle on functional connectome in ageing male and female mice

Houéfa Armelle Lokossou, Giovanni Rabuffo, Monique Bernard, Christophe Bernard, Angèle Viola, Teodora-Adriana Perles-Barbacaru

NeuroImage 290 (2024) 120576

Contents lists available at ScienceDirect

NeuroImage

journal homepage: www.elsevier.com/locate/ynimg

Impact of the day/night cycle on functional connectome in ageing male and female mice

Houéfa Armelle Lokossou [a,b,*], Giovanni Rabuffo [b], Monique Bernard [a], Christophe Bernard [b,*], Angèle Viola [a,1], Teodora-Adriana Perles-Barbacaru [a,1]

[a] Centre for Magnetic Resonance in Biology and Medicine, CRMBM UMR 7339, Aix-Marseille University-CNRS, Marseille, France
[b] Institute of Systems Neuroscience, INS UMR 1106, Aix-Marseille University-INSERM, Marseille, France

ARTICLE INFO

Keywords:
Light/dark cycle
Resting-state fMRI
Functional connectome
Rodent
Sex
Ageing

ABSTRACT

To elucidate how time of day, sex, and age affect functional connectivity (FC) in mice, we aimed to examine whether the mouse functional connectome varied with the day/night cycle and whether it depended on sex and age. We explored C57Bl6/J mice (6♀ and 6♂) at mature age (5 ± 1 months) and middle-age (14 ± 1 months). Each mouse underwent Blood Oxygen-Level-Dependent (BOLD) resting-state functional MRI (rs-fMRI) on a 7T scanner at four different times of the day, two under the light condition and two under the dark condition. Data processing consisted of group independent component analysis (ICA) and region-level analysis using resting-state networks (RSNs) derived from literature. Linear mixed-effect models (LMEM) were used to assess the effects of sex, lighting condition and their interactions for each RSN obtained with group-ICA (RSNs-GICA) and six bilateral RSNs adapted from literature (RSNs-LIT). Our study highlighted new RSNs in mice related to day/night alternation in addition to other networks already reported in the literature. In mature mice, we found sex-related differences in brain activation only in one RSNs-GICA comprising the cortical, hippocampal, midbrain and cerebellar regions of the right hemisphere. In males, brain activity was significantly higher in the left hippocampus, the retrosplenial cortex, the superior colliculus, and the cerebellum regardless of lighting condition; consistent with the role of these structures in memory formation and integration, sleep, and sex-differences in memory processing. Experimental constraints limited the analysis to the impact of light/dark cycle on the RSNs for middle-aged females. We detected significant activation in the pineal gland during the dark condition, a finding in line with the nocturnal activity of this gland. For the analysis of RSNs-LIT, new variables "sexage" (sex and age combined) and "edges" (pairs of RSNs) were introduced. FC was calculated as the Pearson correlation between two RSNs. LMEM revealed no effect of sexage or lighting condition. The FC depended on the edges, but there were no interaction effects between sexage, lighting condition and edges. Interaction effects were detected between i) sex and lighting condition, with higher FC in males under the dark condition, ii) sexage and edges with higher FC in male brain regions related to vision, memory, and motor action. We conclude that time of day and sex should be taken into account when designing, analyzing, and interpreting functional imaging studies in rodents.

1. Introduction

In most species, activity varies on a 24-hour basis known as the circadian rhythm, which is controlled by the main circadian master clock, the suprachiasmatic nucleus, and the coordinated activity of other oscillators in the brain and peripheral tissues (Guilding and Piggins, 2007). The circadian rhythm, which is synchronized by signals from the environment, light being the major zeitgeber of the suprachiasmatic nucleus, controls phases of sleep and arousal, as well as food intake, body temperature, and reproduction. It is affected by the day/night cycle and can be profoundly disrupted in pathological conditions (Steele et al., 2021) and during ageing (Duffy et al., 2015).

MRI studies have revealed a decrease in brain volume during the daytime in young and elderly healthy subjects, as well as in patients with

* Corresponding authors at: Institut des Neurosciences des Systèmes, INS, UMR_S 1106, Faculté de Médecine la Timone, 27 bd Jean Moulin, 13385 Marseille.
E-mail addresses: houefa-armelle.lokossou@univ-amu.fr (H.A. Lokossou), Christophe.BERNARD@univ-amu.fr (C. Bernard).
[1] the authors co-directed this work

https://doi.org/10.1016/j.neuroimage.2024.120576
Received 27 April 2023; Received in revised form 7 March 2024; Accepted 12 March 2024
Available online 13 March 2024

neurological disorders (Nakamura et al., 2015; Trefler et al., 2016), with a greater impact on the frontal and temporal lobes in younger subjects (Trefler et al., 2016). In addition to volumetric changes, variations in BOLD signal were detected with daytime progression using resting-state functional MRI (rs-fMRI) (Farahani et al., 2022, 2021; Orban et al., 2021). Functional connectivity (FC) refers to the statistical dependency between BOLD signals in different brain regions, which can be measured over several minutes at rest (Biswal et al., 1995). In healthy young individuals, FC across the whole brain decreases with daytime progression (Orban et al., 2021), but would not depend on circadian typology (extreme morning-type and evening-type) (Duffy et al., 2015; Farahani et al., 2022, 2021). Similar investigations have been conducted in elderly subjects. Daily rhythmicity was assessed at group-level in healthy elderly and amnesic subjects with mild cognitive impairment, by modeling the temporal evolution of the connectivity strength and the spatial extent of each resting-state network (Blautzik et al., 2014). Healthy elderly subjects showed resting-state networks (RSNs) with high and low rhythmicity comparable to the distribution observed in healthy young subjects. The highly rhythmic networks included a sensorimotor, a cerebellar and a visual network while the less rhythmic networks included a network associated with executive control and an orbitofrontal network. In amnesic patients, the degree of daily rhythmicity was reduced and dysregulated (Blautzik et al., 2014). Moreover, rs-fMRI studies using seed-based analysis or graph theory have shown a more efficient functional neural network organization in people scanned in the evening than in the morning (Farahani et al., 2022, 2021). The somatomotor network presented the most highly connected areas in the evening while the ventral attention and visual networks were more active in the morning (Farahani et al., 2022). Although these studies show that time of day is an independent variable that must be taken into account to correctly interpret rs-fMRI studies in humans, the impact of ageing on the modulation of FC by time of day remains poorly understood (Blautzik et al., 2014; Fafrowicz et al., 2019). The study of the impact of the day/night cycle on brain connectivity is complicated not only by the interindividual variability of the functional connectome (Biswal et al., 2010; Melozzi et al., 2019) but also by its dependence on age and sex (Biswal et al., 2010).

The purpose of this exploratory study was to examine the effects of sex, lighting condition, age, and their interactions on brain dynamics in C57BL6/J mice, a strain widely used in neuroscience research, using rs-fMRI. As neuronal activity changes as a function of the time of day in rodents (Bernard, 2021; McCauley et al., 2020), we hypothesized that resting-state FC should show parallel changes. The functional connectome of male and female mice at two age stages and at different time points during the day/night cycle was assessed using independent component analysis (ICA) or region level analysis followed by linear mixed-effects analyses.

2. Subjects and methods

2.1. Ethics statement

Animal studies followed the French Ministry of Agriculture's guidelines on animal care and the directive 2010/63/EU of the European Parliament and of the Council of 22 September 2010. This project was approved by our institutional committee on ethics in animal research (Comité d'Ethique de Marseille n°14) and authorized by the Ministry of Higher Education, Research, and Innovation (project authorization n° 26779).

2.2. Animals and study design

Specific-pathogen-free 8-week-old C57BL6/J mice (6 females and 6 males) were purchased from Janvier Labs (Le Genest-Saint-Isle, France). The animals were maintained at a temperature of 22–24 °C and humidity of ca 50 % with a 12 h light/12 h dark cycle. They were housed in ventilated cabinets protecting them from possible light and sound pollution during the nocturnal phase. The animals were cared for during working hours. The animals were housed in an enriched environment (nesting material, igloo with saucer wheel, plastic tubes, plastic shelter) with free access to food (standard maintenance diet, SAFE A04 (irradiated), SAFE-lab, Rosenberg, Germany) and water. The irradiated bedding material (spruce wood granulates) was also from SAFE (SAFE BK8–15–10). Health monitoring in the animal house facility was conducted in accordance with FELASA recommendations, using sentinel animals (Mähler Convenor et al., 2014). Randomization was not necessary as all mice were subjected to the same protocol. Blinding could not be applied because the same investigator performed the MRI experiments and all the data processing steps (Percie du Sert et al., 2020).

After a 2-week acclimatization period, a morphological MRI confirmed that they had no brain anomalies. Although critical for the interpretation of results, it is not clear whether sexual maturity (around d35) (Hagan, 2017) or brain maturation age (around d90–100) (Manukian and Kirakosian, 1985) should be used to establish correspondence with human adult age. In this study, we explored animals at 5 ± 1 months and at 14 ± 1 months, i.e. at mature age (mice aged 3–6 months correspond to 20–30 years in humans) and middle-age (mice aged 10–15 months correspond to 38–47 years in humans) (Dutta and Sengupta, 2016; Hagan, 2017). Four animals were scanned per day at different times of either the light or dark conditions (Fig. 1). For the light condition, lights were on from 7AM (Zeitgeber Time (ZT) = 0) to 7PM (ZT = 12). Since changes in resting-state FC over the course of the day have been reported (Orban et al., 2021), mice scanned early in the morning were also scanned in the afternoon and vice versa at an interval of 5–7 days to minimize cumulative effects of repeated anesthesia (Hohlbaum et al., 2017).

To study the animals under the dark condition during working hours, the ventilated cabinet was moved to a separate room where lights were off from 7AM (ZT = 12) to 7PM (ZT = 0) and access strictly restricted for our experimenters. Animal care and handling during the night condition were carried out under infrared light. MRI explorations began after a minimum delay of 14 days to allow mice to adapt to the reversed cycle (Yamaguchi et al., 2013). Each mouse was explored at 2 different times under the dark condition, in 2 MRI spaced 5–7 days apart. When the mice were 14 months old, the acquisitions were repeated starting with the dark condition followed by the light condition and respecting the same delays between the acquisitions (Fig. 1). In summary, each mouse underwent one morphological MRI at 2.5 months of age, 4 rs-fMRI acquisitions at 5 ± 1 months, and 4 rs-fMRI acquisitions at 14 ± 1 months. Handling, restraint, and anesthesia of mice for MRI explorations in the dark condition were performed under infrared light.

2.3. In vivo MRI protocol

Animals were anesthetized with isoflurane 3–4 % in air for induction (Vetflurane, Virbac, Carros, France) and then injected s.c. with medetomidine (Domitor, Virbac, Carros, France) at a single dose of 0.13 mg/kg. The right side of the body was shaved dorsally and ventrally from the tail base to the chest for oximetry. Animal preparation took approximately 10 min.

The MRI protocol was performed on a Pharmascan 70/16 US MRI system operating at 7T (Bruker, Ettlingen, Germany). A linearly polarized volume resonator (72 mm internal diameter) was used for RF transmission in combination with a receive-only 2 × 2-element cryoprobe (< 30 K) (Bruker, Fällanden, Switzerland). Anesthetized mice were placed into a cradle equipped with a stereotaxic head-holder and a nose cone delivering isoflurane (1 % in air). Lubricant eye drops (Ocry-Gel, TVM, Lempdes, France) were applied. A pressure pad was positioned under the abdomen for respiration and an optical fiber-based pulse oximetry sensor was attached to the flank and lower abdomen for real-time monitoring of arterial blood saturation (SpPO2) (MouseOx,

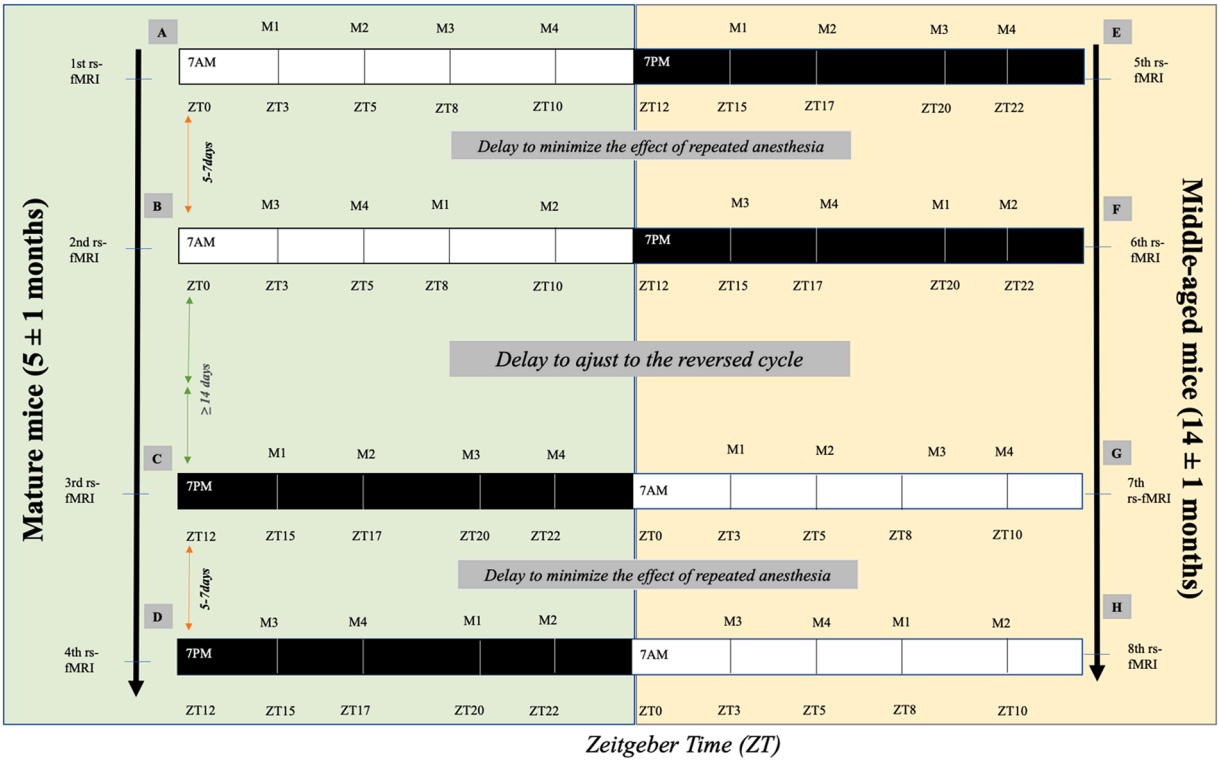

Fig. 1. Experimental design
Under the light condition, lights were on from 7AM (ZT0) to 7PM (ZT12). For the 1rst rs-fMRI exploration, mice M1 to M4 were scanned at ZT3 (M1), ZT5 (M2), ZT8 (M3) or ZT10 (M4) (A). In the 2nd exploration, mice scanned at ZT3 or ZT5 during the 1rst rs-fMRI session were explored later (ZT8 or ZT10) and vice versa. A delay of 5–7 days was observed between the explorations to minimize the effect of repeated anesthesia (B). At the end of the 2nd MRI exploration, the light/dark cycle was reversed (lights off from 7AM to 7PM) to allow the investigator to scan the mice from ZT12 during working time. After a minimum delay of 14 days to allow mice to adapt to the reversed cycle, mice M1 to M4 were scanned under the dark condition. They were explored twice at different times (ZT15, ZT17, ZT20 or ZT22) with an interval of 5–7 days between acquisitions (C-D). Rs-fMRI explorations were performed when the mice were mature (scans 1 to 4) and middle-aged (scans 5 to 8). At middle-age, acquisitions were started under the dark condition followed by the light condition using the same protocol (E-H).

BiosebLab, Vitrolles, France). Body temperature was measured using a rectal optical fiber probe and maintained between 33 and 35 °C with a circulating warm water blanket. This temperature range was chosen to avoid continuous infusion of medetomidine during rs-fMRI acquisitions and to limit the risk of having to increase the percentage of isoflurane. All sensors were connected to an MR-compatible monitoring system (SAII, Stony Brook, NYS). After standard adjustments and acquisition of a localizer scan, a magnetic field map-based shimming (MAPSHIM) protocol was applied within an ellipsoid volume covering the whole brain. Isoflurane was kept below 0.6 % for at least 15 min prior to BOLD acquisitions so that animals were under a combination of light sedation and inhalation anesthesia (Grandjean et al., 2014).

BOLD rs-fMRI experimental data were acquired using a 2D gradient-echo echo-planar imaging (GE-EPI) sequence (40 axial slices, 16 × 16 mm^2 field of view, 110 × 110 matrix, yielding an in-plane voxel size of 0.145 × 0.145 mm^2, 0.40 mm slice thickness, flip angle = 45°, bandwidth = 300 kHz, TR of 2500 ms, TE of 19.91 ms, number of averages = 1, yielding a temporal resolution of 2.5 s, with ghost correction duration of 0.7 ms). Partial Fourier imaging was applied with a value of 1.2 in phase encoding direction. The duration of the image time series was 22 min for 512 acquired repetitions. Rs-fMRI acquisitions were performed with higher spatial resolution and lower temporal resolution compared with most other studies (Bajic et al., 2017; Grandjean et al., 2020) but similar to previously published work by Melozzi and colleagues (Melozzi et al., 2019). Acquisitions were repeated in the event of animal motion detected by the pressure pad.

2.4. Rs-fMRI preprocessing

Raw data were converted to nifti-format using a script under MIPAV v.10.0.0. The script opens Bruker images (2dseq reconstructed in 16-bit signed format under Paravision 6), reorganize them into 512 vol with 40 slices each and scales up the dimensions by a factor of 10. The 4D rs-fMRI was cloned and the first volume was extracted to serve as the anatomical reference image; the image type was changed to “float” before the next step. The 3D rs-fMRI stack was blurred by a gaussian kernel of 10 mm after scaling. The original 3D rs-fMRI stack was corrected for bias field by dividing by the blurred image. The resulting image was multiplied by 1000 before converting to “short” type.

As there is no standardized pipeline for preprocessing mouse brain rs-fMRI data, each laboratory must adapt its own pipeline to the quality of the data acquired. As the usefulness of certain preprocessing procedures (white matter and cerebrospinal fluid signal regression, global signal regression) is still debated (Bartoň et al., 2019; Birn, 2012; Fox and Raichle, 2007; Gawryluk et al., 2014; Murphy et al., 2009), it was assessed (data not shown) before deciding on our pipeline. The different steps retained were in agreement with the literature (Bajic et al., 2017) and were validated not only on our datasets but also on external datasets (https://openneuro.org/datasets/ds001591/versions/1.3.0).

All further preprocessing steps were performed using FSL’s recommended preprocessing pipeline from FMRIB’s Software Library (FSL version 6). Data with significant head motion detected by visual inspection were discarded. Preprocessing included identification of motion-affected volumes using the frame displacement (FD) metric (Power et al., 2012) with a threshold set to 70 μm after scaling. The volumes affected by motion were regressed out to eliminate their

influence on the BOLD signal and avoid any bias on the results. After this step, all rs-fMRI data were registered onto the first rs-fMRI volume which corresponds to the registration to native space. The Brain Extraction Tool (BET) was applied to the data to remove non-brain tissue before applying a bias field correction step to the 4D skull-stripped data (Smith, 2002). Slice-timing correction using phase-shift of the time-series in the frequency domain, grand-mean intensity normalization of the entire 4D dataset by a single multiplicative factor and high pass temporal filtering (0.01 Hz) were performed using FEAT (FMRI Expert Analysis Tool, version 6.00, part of FSL) (Woolrich et al., 2004).

Sudden changes in intensity in the filtered 4D dataset were detected using the default FSL DVARS (Power et al., 2012) metric threshold (the temporal derivative root mean square variance; the 75th percentile +1.5 × interquartile range) and regressed out. Then, global signal regression and low pass filtering (0.1 Hz) were applied and data were registered to the Allen template using FLIRT (FMRIB's Linear Image Registration Tool) followed by nonlinear (FNIRT, FMRIB's Nonlinear Image Registration Tool) warping (Jenkinson et al., 2002a).

2.5. Rs-fMRI post-processing

2.5.1. Group independent component analysis

We performed group-ICA for: 1) male mice under the light condition only; 2) mature male and female mice in both lighting conditions; and 3) middle-aged female mice only, under the light and dark conditions. Group-ICA is an approach that allows the temporal concatenation of the entire set of rs-fMRI data across all subjects to identify independent component (IC) maps common to the group. Spatial smoothing by a Gaussian kernel and an isotropic resampling resolution of 4 mm (0.4 mm in the original resolution) were applied to the preprocessed data for multi-session temporal concatenation followed by Probabilistic ICA (Beckmann and Smith, 2004) as implemented in MELODIC GUI (Multivariate Exploratory Linear Decomposition into Independent Components, version 3.15, part of FSL). For each group, 40 IC maps were extracted from which plausible RSNs **(RSNs-GICA)** were identified on the basis of the following criteria: unilateral or bilateral IC limited to the brain and consistent with the literature (Bukhari et al., 2017).

- **Linear mixed-effects models (LMEM) using RSNs-GICA in mature mice**

To assess the main effects of sex, age, and lighting condition as well as the effect of their interactions, the averaged time series defined by the mask of each plausible RSN-GICA was extracted for each subject. Data processing was performed using FEAT (FMRI Expert Analysis Tool) Version 6.00, part of FSL (Woolrich et al., 2004). The first-level analysis consisted of registration to high resolution standard space images using FLIRT (FMRIB's Linear Image Registration Tool) (Jenkinson et al., 2002b) followed by pre-statistics processing. Time series statistical analysis was carried out using FILM (FMRIB's Improved Linear Model) with local autocorrelation correction (Woolrich et al., 2001). A seed-based connectivity map of each mask was generated for each subject in the groups of mature male and female mice. In the second-level analysis, fixed-effects analyses were performed to obtain the averaged BOLD signal of the two rs-fMRI acquisitions performed under the same condition (light or dark) in each subject. The third-level analysis was carried out using FLAME 1 (FMRIB's Local Analysis of Mixed Effects) to generalize the findings to the population, taking into account missing scans. Z statistic images were thresholded using clusters determined by $Z > 3.1$ and a (corrected) cluster significance threshold of $P \leq 0.001$ (Worsley, 2001).

- **Dual regression analysis to assess the effects of the light/dark cycle in middle-aged female mice**

After group-ICA in middle-aged females, Dual Regression (DR), a mathematical method that utilizes the IC maps as network templates to identify the corresponding FC maps in each subject, was used for the middle-aged female group. In the first stage of DR, subject-specific time courses for each template network were extracted using a multivariate spatial regression of the template maps against each subject rs-fMRI data. In the second stage, the subject-specific time courses from stage 1 were used in a second multivariate regression against the subjects' rs-fMRI data to identify the subject-specific maps corresponding to each network template of interest (Nickerson et al., 2017). We used DR (v0.6) for between-subject analysis that allows voxel-wise comparisons of rs-fMRI data (Filippini et al., 2009; Nickerson et al., 2017; Veer, 2010). A permutation-based non parametric inference analysis (Nichols and Holmes, 2002) was performed with subject-specific IC maps concatenated across subjects and submitted to voxel-wise between-subject analysis testing for the effect of the light and dark conditions using FSL-*randomise* permutation-testing tool (Winkler et al., 2014). FSL's general linear model (GLM) was used to define the design of the contrasts testing day/night alternation effects within the group of middle-aged female mice. For this analysis we ran 5000 randomized permutations as recommended to reduce uncertainty, while threshold-free cluster enhancement (TFCE) (Smith and Nichols, 2009) was used for statistical inference to validate the likelihood of extended areas of signal, which also considers information from neighboring voxels. Correction for multiple comparisons across space was applied using permutation testing and TFCE.

2.5.2. Region-level analysis using common RSNs adapted from the literature (RSNs-LIT) followed by LMEM

We generated FC matrices to visualize correlation patterns between networks. FC was derived from region-level analysis, which was obtained by registering BOLD signals onto a parcellation of the Allen Mouse brain atlas. The parcellation was extracted through the Allen Connectivity Builder interface of The Virtual Mouse Brain pipeline (Melozzi et al., 2017), and consisted of 148 regions of interest (ROIs) from which we excluded 40 regions known to produce artefacts according to the Allen Institute (the cerebellum, midbrain, brainstem and olfactory bulb) (suppl. Table 1).

For each mouse, we calculated the FC (108 ROIs × 108 ROIs correlation matrices). The FC matrix is defined as Pearson's correlation (r) between any pair (i,j) of BOLD signals $x_i(t)$ and $x_j(t)$, i.e., $FC(i,j) = r(i,j) = \langle z_i(t) \cdot z_j(t) \rangle_t \equiv \langle E_{ij}(t) \rangle_t$, where $z(t) = (x(t) - \mu)/\sigma$ is the z-scored time series for a signal $x(t)$ with mean μ and standard deviation σ. The element-wise product of the z-scored signals for regions (nodes) i, j is defined as the "edge co-activation" time series $E_{ij}(t)$.

The 108 ROIs were grouped according to six common bilateral RSNs (Default Mode Network **DMN**, Visual network **Vis**, Lateral Cortical Network **LCN**, Basal Forebrain **BF**, Hippocampal Formation **HPF**, Thalamus **Th**) obtained by visual adaptation from previous work on the RSN organization of the mouse brain (Liska et al., 2015). We averaged the FC for each RSN and obtained a 6 × 6 matrix. This corresponded to 21 unique pairs of RSNs (or "edges") for the *FC* matrix.

Since we had no exploitable rs-fMRI acquisitions for males at middle-age, we performed data consolidation and introduced a new variable named 'sexage': mature females (F_M); mature males (M_M); middle-aged females (F_MA). We used the "edges" as variable and assigned it the corresponding FC value. This allowed to keep the three groups and increased the number of observations per lighting condition. Then, we carried out LMEM to check for the effects of sexage, lighting condition, and edges, and their interactions on *FC* considering the variability induced by each mouse on our model. LMEM analyses were followed by post-hoc Tukey multiple comparison tests under RStudio, version 4.3.2. Significance was set to $p < 0.05$.

2.6. Elapsed time under the light condition or the dark condition and assessment of physiological parameters

The time spent under the light condition or the dark condition before starting rs-fMRI explorations was assessed for each mouse and mean and standard deviation (SD) were compared between groups using the non-parametric paired Wilcoxon test or the unpaired Mann-Whitney test. The non-parametric Kruskal-Wallis test was used when comparing the groups for the light condition or the dark condition. Respiratory rate, rectal temperature and blood oxygen saturation were compared between male and female mice using Mann-Whitney test. Significance was set to $p < 0.05$.

3. Results

3.1. Mice follow-up

In addition to a short anesthesia at 2.5 months for a morphological assessment, mice were submitted to 4 anesthesia sessions at each time point of the follow-up (5 and 14 months of age) of 75 min each, with the four sessions separated by a time interval of 5 to 7 days. Respiratory rate, blood oxygen saturation and rectal temperature were not significantly different between mature females and males across MRI explorations (suppl. Table 2). In a few cases, we were unable to obtain reliable continuous oximetric recordings.

At 5 months of age, the mean weight of the animals was 34.16 ± 3.20 (SD) g for males and 23.30 ± 2.28 (SD) g for females and at 14 months 38.75 ± 2.63 (SD) g and 26.09 ± 1.97 (SD) g, respectively. Weight gain during the 9-month interval between follow-up points was 13.42% for males and 11.93% for females.

One male mouse developed severe dermatitis, a frequent condition in the C57Bl/6 strain and had to be euthanized. The first rs-fMRI exploration at 5 months was carried out without any anesthetic complication. However, from the 2nd rs-fMRI exploration onwards for female mice and from the 4th rs-fMRI exploration onwards for male mice, unexpected respiratory distress occurred either on induction of anesthesia or during maintenance resulting in the sudden death of 2 male and 2 female mice. Human error or malfunction of the anesthetic system were both discarded. At 14 months, the same problem occurred, and 3 males and 2 females died under anesthesia. In the end, only two females completed the follow-up.

3.2. Assessment of image quality

The number of usable acquisitions per time point for mature and middle-aged mice is given in Table 1. Apart from distortions near air-bone interfaces and ghost artefacts in caudal and rostral slices (suppl. Fig. 1), the other slices were of good quality (signal-to-noise ratio > 56). The dorso-ventral signal intensity gradient due to the surface cryoprobe was corrected during data preprocessing. Rs-fMRI acquisitions with significant artefacts due to head motion or physiological instability were discarded from the analyses (females, n = 7; males, n = 8).

Due to the removal of several acquisitions from the analyses, the scans performed under the same lighting condition for each age and sex were grouped (Table 1).

3.3. Elapsed time under the light condition or the dark condition before the beginning of rs-fMRI explorations

Rs-fMRI acquisitions were performed 6 to 8 h after switching lights on or off. No significant difference was found between the time elapsed under the light condition or the dark condition within both sexes and age groups (Table 2).

3.4. Reliability of RSNs under the light condition

Since we had more data at both time points of the light condition for the group of mature male mice, we compared the 12 RSNs found for this group after the temporal concatenation of IC with those reported in the literature as a first quality check and found similarities using anatomical landmarks. Since some RSNs found in the light condition were consistent with those described in the literature (suppl. Table 3), we considered our ICA approach to be validated and rs-fMRI data under the light and dark conditions were pooled to perform group-ICA for mature and middle-aged female mice.

3.5. Main results derived from group-ICA

3.5.1. Main effects of sex, lighting condition and their interactions on RSNs in mature mice

We found 16 plausible RSNs in mature male and female mice under the light and dark conditions after group-ICA. These networks involved cortical structures, the hippocampus, thalamic and hypothalamic regions, the pineal gland, the reticular nucleus of the midbrain and cerebellar regions (Fig. 2; Table 3).

Linear mixed-effect analyses revealed no significant effect of lighting condition or interaction effect with sex on RSNs-GICA.

A significant effect of sex was detected ($p < 0.001$) for the IC33 network comprising the retrosplenial and primary visual cortices, the superior and inferior colliculi, the hippocampus, the periaqueductal gray, the thalamic and cerebellar regions of the right hemisphere. Group-analysis showed a strong correlation between the network and ipsilateral regions in females whereas strong correlations were detected with contralateral regions in male mice independent of lighting

Table 2
Mean and standard deviation of time spent under the light condition and the dark condition at the beginning of rs-fMRI exploration and corresponding Zeitgeber time (ZT). Mann-Whitney unpaired test was used to compare light and dark conditions in each group and thereafter, Kruskal Wallis test was performed to compare male and female groups for the light and dark conditions.

Mice	Conditions		
	Light	Dark	P-values
Mature ♂	6h12 ± 2h27 min ZT6 ± 2h27 min	5h45 ± 2h54 min ZT17 ± 2h54 min	0.63[a]
Mature ♀	8h22 ± 2h40 min ZT8 ± 2h27 min	7h49 ± 2h19 min ZT19 ± 2h519 min	1[a]
Middle-aged ♀	7h44 ± 2h42 min ZT8 ± 2h27 min	7h48 ± 2h45 min ZT19 ± 2h519 min	0.70[a]
P-values	0.16[a]	0.25[a]	–

[a] non-significant.

Table 1
Number of usable acquisitions per time point for mature and middle-aged mice.

		Usable acquisitions					
Age	Sex	[ZT0-ZT5]	[ZT6-ZT11]	**[ZT0-ZT11]**	[ZT12-ZT17]	[ZT18-ZT23]	**[ZT12-ZT23]**
Mature group	Male	6	6	**12**	3	2	**5**
(5 ± 1 months)	Female	2	6	**8**	1	3	**4**
Middle-aged group	Male	0	0	**0**	0	0	**0**
(14 ± 1 months)	Female	2	2	**4**	2	3	**5**

Zeitgeber Time (ZT); ZT0 = light on at 7AM and ZT12 = light off at 7PM.

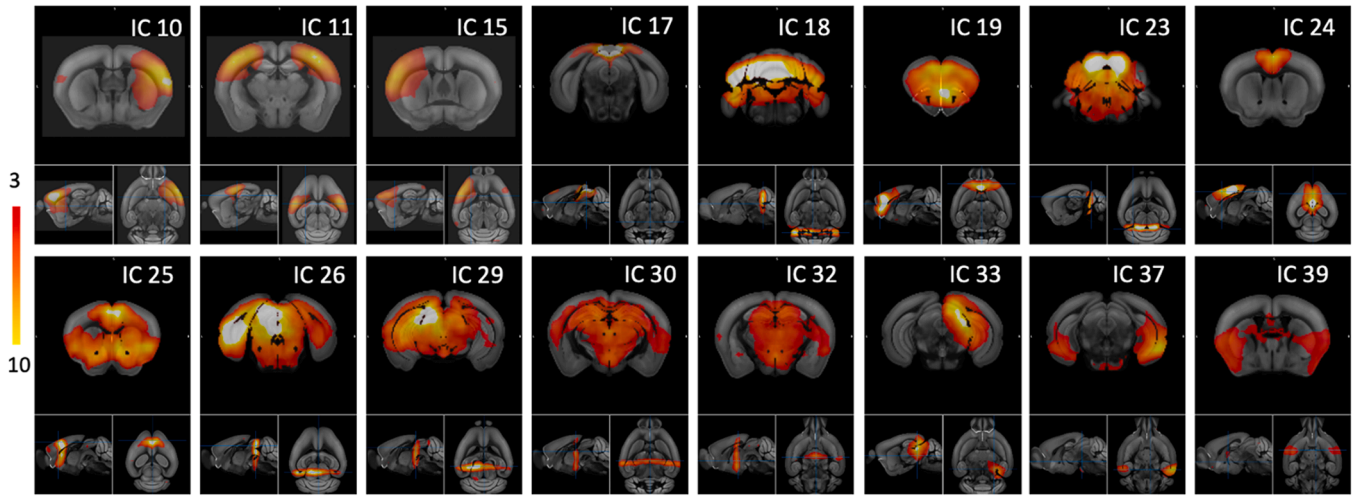

Fig. 2. Sixteen plausible RSNs in mature female and male mice under the light and dark conditions after group-ICA. The networks are unilateral or bilateral including cortical, subcortical, and cerebellar regions. Z-score color maps are overlaid on the Allen template (axial and smaller orthogonal views are shown). Z-scores were >3.

condition. Significant clusters found in mature males were located in the left hemisphere in the hippocampus (CA1, dentate gyrus), retrosplenial cortex, superior and inferior colliculi, and cerebellar regions (left simple lobule, lobules II, IV and V) (Fig. 3).

Network laterality was confirmed using seed-based analysis (SBA) with males showing bilateral RSNs and females unilateral RSNs using two different ROIs (suppl. materials, suppl. Figs. 3 and 4).

3.5.2. *Main effects of age, lighting condition and their interactions*

Due to the death of male mice at 14 months and the limited number of usable acquisitions in middle-aged females, we assessed neither the age-related changes in brain activity nor the effects of the interactions between age and lighting condition in RSNs-GICA.

We then concatenated data from middle-aged female mice under the light and dark conditions and compared the two groups using FSL's permutation-testing tool called randomise. Multi-session temporal concatenation ICA led to the identification of 11 RSNs-GICA (Table 4). These networks included cortical, hippocampal, thalamic, hypothalamic, and cerebellar regions. Some networks were unilateral, with the contralateral structures involved in other networks. Using DR and randomization analyses, a significant difference between the light and dark conditions was found in network 37 (Fig. 4), at the level of the pineal gland exhibiting a higher activity under the dark condition as compared to the light condition (Fig. 5).

SBA confirmed the significant interactions between the pineal gland, retrosplenial cortex and visual cortex (suppl. materials; suppl. Fig. 2) found during group-ICA (Fig. 4).

3.6. *Main results obtained from region-level analysis of six common RSNs derived from the literature*

The mean FC were summarized for each pair of RSN-LIT regardless of sexage and lighting condition (Fig. 6) and for each sexage by condition (suppl. Figs. 5 and 6).

In our model, the interindividual variability of *FC* was 11 %. LMEM analyses revealed no significant effect of lighting condition, sexage, lighting condition×edges or sexage×lighting condition×edges on *FC* but significant effects of edges ($p < 2.2 \times 10^{-16}$), sexage×edges ($p = 0.009$) and sexage×lighting condition ($p = 0.013$) on *FC*. The FC depended on edges and connections between brain regions were stronger in mature males than in mature females independent of lighting condition mainly within HPF and between HPF-Th and Vis-HPF (Fig. 7). When examining the interaction effects between sexage and lighting condition, mature females displayed higher FC under the light condition compared to the dark condition, and vice versa for mature males. Paired multiple comparisons tests showed that FC was significantly higher in mature males ($p = 0.049$) than in mature females under the dark condition for connections within Vis, Th, LCN, HPF and between Vis-HPF and HPF-Th (Fig. 8).

4. Discussion

The aim of our study was to determine whether resting-state network activity and interactions between RSNs in mice, using BOLD signal-derived FC as a proxy, changed during the day/night cycle as a function of age and sex.

We identified for the first time the RSNs associated with the day/night cycle in mature and middle-aged mice using group-ICA. We found a main effect of sex in a RSN-GICA involving the right hemisphere in mature mice, and changes in brain activity depending on lighting condition in middle-aged female mice. In addition, we detected networks resembling the DMN, somatosensory, autonomic, subcortical and thalamic networks not only in IC maps derived from mature male mice under the light condition (as a first quality check), but also in IC maps derived from other groups under the light and dark conditions. These findings are consistent with previously published networks in rodents (Bajic et al., 2017; Bukhari et al., 2017; Grandjean et al., 2020; Mandino et al., 2022; Zerbi et al., 2015). We also identified candidate networks for the limbic network and the sensorimotor, cerebellar, visual, and executive control networks in line with those already reported in humans scanned at different times of the day (Blautzik et al., 2014). However, these networks showed some differences with human networks because of anatomical homology issues between humans and mice and because some RSNs sometimes included structures other than those involved in known networks (Tables 3 and 4 and suppl. Table 3). Using region-level analysis, we showed that FC varies with sexage and pairs of RSNs as well as with sexage and lighting condition.

4.1. *Effect of sex, lighting condition and their interactions on RSNs in mature mice*

Learning-dependent timing, procedural memory formation and spatiotemporal predictions of motor actions are controlled at least in part by the cerebellum (De Zeeuw and Ten Brinke, 2015; Stoodley, 2012) and are facilitated by sleep (Verweij et al., 2016). The cerebellum is reciprocally connected with the cerebral cortex and the reverberating activity in this loop depends on the sleep-wake state. Connectivity studies in humans reveal that the FC within the cortico-cerebellar

Table 3
Overview of the main anatomical regions identified in the selected IC maps (the different networks) in mature male and female mice under the light and dark conditions and comparison with the potential homologous networks in humans (Ω) or rodents (α). The corresponding networks in the literature did not include the structures in brackets.

Networks in middle-aged female mice	Structures	Potential homologous networks in literature
Network 10	Right primary motor cortex Right primary somatosensory cortex Left Supplemental somentosensory cortex (Right caudoputamen)	Lateral cortical network α (Mandino et al., 2022)
Network 11	Primary somatosensory cortex Caudoputamen Hippocampus Retrosplenial cortex, lateral agranular	Sensorimotor network
Network 15	Left primary motor cortex Left primary somatosensory cortex Left Supplemental somentosensory cortex (Left caudoputamen)	Lateral cortical network α (Mandino et al., 2022)
Network 17	Superior colliculus Pineal gland Retrosplenial cortex Primary visual cortex	Visual network α Ω (Blautzik et al., 2014; Zerbi et al., 2015)
Network 18	Lingula Lobules II-III- IV-V Crus I Simple lobule	Cerebellar network α (Zerbi et al., 2015)
Network 19	Primary motor cortex Secondary motor cortex Agranular insular cortex Orbital cortex Anterior olfactory nucleus	Part of Default Mode network
Network 23	Inferior colliculus Lobules II-IV-V Simple lobule	Cerebellar network α (Zerbi et al., 2015)
Network 24	Secondary motor cortex Anterior cingulate cortex	Part of Default Mode network
Network 25	Secondary motor cortex Anterior cingulate cortex Cauoputamen Nucleus accumbens Piriform cortex Agranular insular cortex	Sensory visual and auditory networks α (Zerbi et al., 2015)
Network 26	Retrosplenial cortex Subiculum Presubiculum Postsubiculum Entorhinal cortex Primary visual cortex Midbrain reticular nucleus	Hippocampo-Mesencephalo-Pontine Networks **(HMPN)** [a]
Network 29	Hippocampus Retrosplenial cortex Auditory cortex Left entorhinal cortex Superior colliculus Midbrain reticular nucleus Red nucleus	Hippocampo-Mesencephalo-Pontine Networks **(HMPN)** [a]
	Periaqueductal gray Hypothalamic nuclei	
Network 30	Hippocampus Thalamus Primary somatosensory cortex Auditory cortex Tempral association cortex Ectorhinal cortex	Sensory auditory networks α (Zerbi et al., 2015)
Network 32	Hippocampus Thalamus nuclei Hypothalamic nucleus Right caudoputamen Right agranular insular cortex	Limbic network
Network 33	Right retrosplenial cortex Right superior colliculus Right inferior colliculus Right primary visual cortex Right hippocampus Right periaqueductal gray Right cerebellar regions	Right Hippocampo-Thalamo-Mesencephalo-Visuo-Cerebellar Network **(RHTMVCN)**[a]
Network 37	Hippocampus Entorhinal cortex Ectorhinal cortex	Hippocampo-Amygdalo-Entorhinal Network **(HAEN)**[a]
Network 39	Piriform cortex Endopiriform cortex Caudoputamen	Thalamo-Caudo-Amygdalo-PiriformNetwork **(TCAPN)**[a]

[a] New RSNs identified in this study.

network remains intact during sleep, but its strength depends on the stage of sleep and the brain regions involved (Canto et al., 2017). Posterior cerebellar regions have been shown to play a role in the recognition, appraisal, and response to emotional stimuli (Pierce et al., 2023). The retrosplenial cortex is involved in memory formation (Todd et al., 2019); spatial navigation (Cooper and Mizumori, 2001); associative learning (Keene and Bucci, 2008) while the hippocampal CA1 plays a role in memory integration and inference (Schlichting et al., 2014). The visual cortex is important for visual control of action and requires projections from thalamic nuclei (Murakami and Ohki, 2023). The thalamus is an important hub that plays a role in maintaining various cognitive functions (Roy et al., 2022) and in consciousness (Bell and Shine, 2016). Given the structures involved in network 33 (cortex, hippocampus, thalamus, midbrain, and cerebellar structures), we propose that this RSN-GICA plays a role in vigilance states, decision-making, memory and sensory processing during the day/night cycle.

The higher brain activity in male mice than in females in the left cerebellum (lobules III, IV and V), left superior colliculus and hippocampal regions, regardless of the lighting condition is consistent with sex-differences in brain activity (male > female) in the cerebellum during long-term memory (Spets et al., 2021), shelter-direction (Campagner et al., 2023) and with increased neuronal activation in dentate gyrus and CA1 in male mice (Colon and Poulos, 2020). The involvement of both hemispheres in males for this RSN-GICA suggests a better interhemispheric FC in males than in female mice. Although we did not assess the stage of the estrous cycle in our mice, this distinct laterality of the network appears to reflect the effects of hormones on interhemispheric FC in mature females as demonstrated in humans (Pletzer and Harris, 2018) and confirmed for many other RSNs in mice under the light and dark conditions (see suppl. Figs. 3 and 4).

For RSNs from the literature, it was not possible to assess

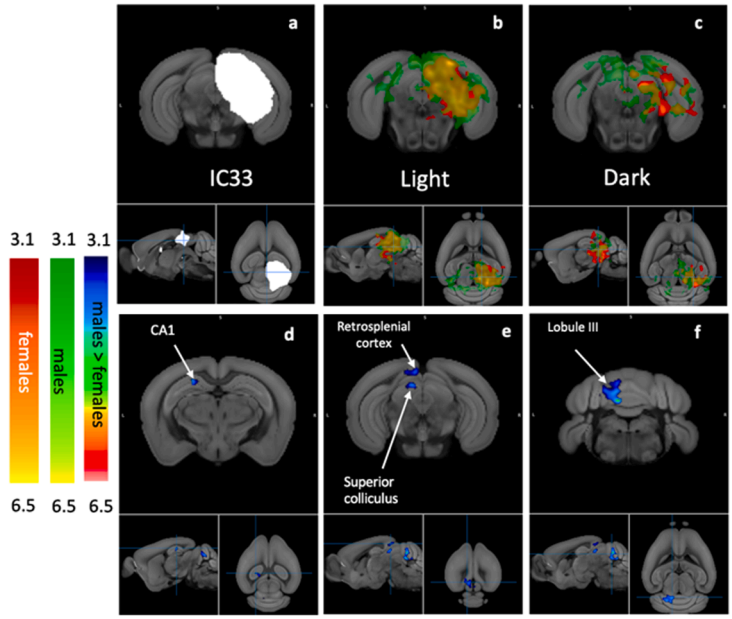

g

Cluster Index	Voxels	P	Z-max intensity	Z-max X	Z-max Y	Z-max Z
2	1091	3.58e-06	4.66	49	22	48
1	677	0.000246	4.01	49	43	58

h

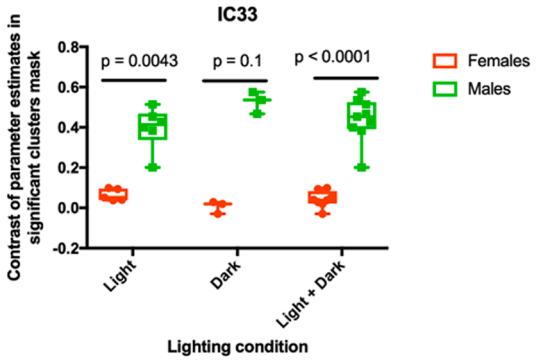

Fig. 3. Sex-related differences in brain activation in RSN-GICA IC33 in mature mice under the light and dark conditions. The average time series from the region defined by the mask of IC33 (white pixels in a) was extracted for each subject as well as brain regions whose activity correlated with the average of IC33 activity. Group average in females (red pixels) and males (green pixels) were obtained under the light (b) and dark conditions (c). Linear mixed-effect models revealed significant effect of sex for 2 clusters (g) in the left superior colliculus, hippocampus, cortical, and cerebellar regions (blue clusters, arrows in d to f) with males showing higher brain activity than females irrespective of lighting condition (h). Z-score color maps are overlaid on the Allen template (axial and smaller orthogonal views are shown). Z-scores were >3.1.

connectivity with the midbrain and cerebellum, as these regions were excluded due to possible artifacts. However, the higher brain connectivity between HPF, Th, Vis in mature males as compared to mature females seems to reflect the connections within network 33 obtained after group-ICA and the significant sex-dependent changes in FC. In addition to the tendency for FC to decrease from the light to the dark condition in females, which is reversed in males, the higher connections between Vis, HPF, Th and LCN under the dark condition (active phase) in mature males compared to females could be linked to sex-related changes in memory consolidation, decision-making and motor actions. We suggest that our findings reflect the divergent learning strategies adopted by males and females (Chen et al., 2021) that change with light/dark alternation.

4.2. *Effect of the day/night cycle on FC in middle-aged female mice*

In our study, the middle-aged female mice showed a significant increase in brain activity in the pineal gland under the dark condition, a finding apparently consistent with its nocturnal function of melatonin production (Macchi and Bruce, 2004; Sapède and Cau, 2013) which is suppressed by light. Although the C57Bl/6 mouse strain is deficient in pineal melatonin due to mutations affecting two enzymes involved in melatonin synthesis (Ebihara et al., 1986; Goto et al., 1989; Kasahara et al., 2010), several studies have detected low but measurable amounts of pineal hormone (Conti and Maestroni, 1996; Vivien-Roels et al., 1998; von Gall et al., 2000). Pineal melatonin is a signal of night and night length, and is also involved in the synchronization of biological rhythms (Arendt and Skene, 2005) and physiological processes, including reproductive function and ageing (Pierpaoli and Regelson, 1994; Vivien-Roels et al., 1998). While melatonin is thought to play a beneficial role in some sleep disorders in humans (Moon et al., 2022), an effect on the sleep of nocturnal rodents seems unlikely since it is released during their most active phase. A phase of temporary increase in pineal melatonin has been described in perimenopausal female rats, in agreement with human findings (Okatani et al., 2000, 1999). These studies showed that melatonin levels were significantly higher at 16 months in perimenopausal animals than in premenopausal rats at 12 months, and would be linked to the fall in estrogen. Although we did not check the estrous cycle, our middle-aged mice should be in a period of reduced estrous cycles, with menopause occurring between 13 and 16 months of age in the C57BL/6 J strain (Nelson et al., 1982).

In melatonin deficient animals producing low amounts of pineal hormone, and in the absence of pineal melatonin and estradiol assays it is difficult to establish a causal link with the activation detected by rs-fMRI. We assume that nocturnal activation of the pineal gland in middle-aged melatonin-deficient female mice probably reflects activation of signaling pathways relaying photic information upstream of melatonin synthesis. Interestingly, these pathways are also known to express estrogen receptors (Bailey and Silver, 2014). The implication of the pineal gland in a network including the visual cortex is consistent with the processing of photic information by these structures, the mean FC of the visual cortex being reduced under the dark compared to the light condition (suppl. Fig. 6). The finding of the retrosplenial cortex in the same network reflects its connection with the visual cortex and its role in the integration of sensory information (Powell et al., 2020).

This is the first study to report pineal gland activity in resting-state networks. Indeed, MRI visualization of the pineal gland in mice is difficult due to its location and surrounding structures (Langevad et al., 2014). In this study, the good spatial resolution of our rs-fMRI acquisitions and the dual regression analysis using the IC maps derived from the group analysis allowed the pineal gland to be identified. The advantage of the ICA method is that the data can be analyzed without any prior knowledge and that it allows the FC of the entire brain to be investigated. Moreover, seed-based analysis confirmed the correlations between the pineal gland, retrosplenial and visual cortex in middle-aged females (see suppl. Fig. 2). The use of RSNs-LIT not including the pineal gland did not allow confirmation of ICA findings.

4.3. *Effects of body temperature on BOLD signal and functional connectivity*

Core-body temperature is 1 °C higher than deep brain temperature in

Table 4
Overview of the main anatomical regions identified in the selected IC maps (the different networks) in middle-aged female mice under the light and dark conditions and comparison with the potential homologous networks in humans (Ω) or rodents (α). The corresponding networks in the literature did not include the structures in brackets.

Networks in middle-aged female mice	Structures	Potential homologous networks in literature
Network 14	Inferior colliculus	Cerebellar network [α] (Zerbi et al., 2015)
Network 15	Subiculum Enthorhinal cortex Visual cortex Superior Colliculus	Hippocampo-Mesencephalo-Pontine Networks **(HMPN)** [a]
Network 17	Insular cortex Left secondary somatosensory cortex	Lateral cortical network [α] (Mandino et al., 2022)
Network 18	Limbic cortex Cingular cortex Motor cortex	Cingulo-Medio-Frontal Network (**CMFN**)[a]
Network 20	Right Primary motor cortex Right Insular cortex Primary somatosensory cortex	Lateral cortical network [α] (Mandino et al., 2022)
Network 25	Anterior cingulate cortex Caudoputamen Prelimbic cortex Motor cortex Piriform cortex	Fronto-Parieto-Limbic Network **(FPLN)** [a]
Networks 27 and 29	Retrosplenial cortex Primary visual cortex Right lateral visual cortex (Right Subiculum) (Right hippocampus)	Visual network [α Ω] (Blautzik et al., 2014; Zerbi et al., 2015)
Network 31	Superior colliculus Left Retrosplenial cortex Left Primary visual cortex (Left subiculum)	Visual network [α Ω] (Zerbi et al., 2015)
Network 32	Visual cortex Retrosplenial cortex Primary auditory cortex Temporal auditory cortex Perirhinal cortex	Sensory visual and auditory networks [α] (Zerbi et al., 2015)
Network 37	Visual cortex Retrosplenial cortex Pineal gland	Visual network [α Ω] (Blautzik et al., 2014; Zerbi et al., 2015)

[a] New RSNs identified in this study.

small anesthetized animals and decreases by 3–4 °C towards the cortical surface (Zhu et al., 2006). Furthermore, with agents such as isoflurane, cortical brain temperature can be 10 °C cooler than body temperature (Kalmbach and Waters, 2012). In this study, body temperature was maintained between 33 and 35 °C. Cortical and deep brain temperature were therefore below 33 °C. A previous study showed that a high temperature (37–39 °C) can modify the BOLD signal and change the connections between regions (Vanhoutte et al., 2006), while reducing the temperature from 38 to 24 °C increases the BOLD signal by 35 to 44 % during in-vivo neuroimaging (Harris et al., 2018). Consequently, the BOLD signal should be higher under our experimental conditions in comparison with published studies performed at higher temperature. The identification of networks already documented in the literature confirms that maintaining the animals at lower body temperature does not suppress brain activity in those networks and provides results comparable to those obtained at a higher temperature. Nevertheless, we cannot exclude the possibility of changes in connectivity strength linked to body temperature (Vanhoutte et al., 2006).

4.4. Effects of anesthesia on brain function

General anesthesia is a reversible state characterized by loss of consciousness, amnesia, analgesia, immobility (in response to pain stimuli) and hemodynamic stability with control of the stress response (Brown et al., 2010; Purdon et al., 2009). Anesthesia reduces neurotransmission (Angel, 1993; Campagna et al., 2003) and has a neuroprotective effect in adult rats but a neurotoxic effect in newborn and aged rats (Neag et al., 2020). Anesthesia reduces cortico-cortical connectivity in brain networks such as the DMN (Greicius et al., 2008; Jordan et al., 2013), salience network (Guldenmund et al., 2013) and executive control network (Boveroux et al., 2010), and restricts and lateralizes subcortical FC (Nir et al., 2022). The effects of four commonly used anesthetics (isoflurane, medetomidine, propofol and urethane) on FC were compared (Grandjean et al., 2014). The findings suggest that the combination of low doses of medetomidine and isoflurane preserve strong correlations within cortical and subcortical structures in mice. The anesthetic regimen used in this study was based on this recommendation.

Although general anesthesia is thought to induce a state similar to non-rapid eye movement (NREM) sleep (Murphy et al., 2011), rs-fMRI studies comparing general anesthesia and natural sleep yielded conflicting results, depending to a certain extent on the anesthetics used (Guldenmund et al., 2017; Heine et al., 2012; Larson-Prior et al., 2009; Stamatakis et al., 2010). Furthermore, seed-based whole brain FC maps in humans showed marked differences between sleep and general anesthesia: sleep relies primarily on brainstem and frontal lobe function, while anesthesia affects widespread functional networks (Li et al., 2018). Significant decreases in FC were detected during sleep regardless of age, but older subjects showed a lower disconnection during sleep than young subjects (Daneault et al., 2021). It would have been interesting to compare the effects of natural sleep and light anesthesia on the rs-fMRI data of mice under the light and dark conditions during the follow-up period. However, the stress induced by head fixation to scan awake mice may be an independent variable likely to act as a confounding factor (Melozzi et al., 2019).

4.5. Effects of sedation and anesthesia on mouse physiology

A time shift of circadian rhythm has been shown after general anesthesia depending on the day/night cycle (Gökmen et al., 2017; Poulsen et al., 2018) and may affect behavior and physiology. In this study, we did not perform any behavioral tests that could have revealed such a phase shift.

Anesthesia may also affect the well-being of mice (reduced burrowing and nest building behavior in both sexes, slight short-term impairment of food intake in female mice) during the immediate post-anesthetic period (Hohlbaum et al., 2017). A reliable indicator of animal well-being during the follow-up is the body weight. In our study, despite repeated anesthesia, the mice gained approximately 12 % of their body weight over a 9 months interval, which is comparable to the weight dynamics obtained from the mouse breeder (Janvier Labs).

Our study also showed sex- and age-related differences in sensitivity to anesthesia, consistent with a modulation of α2-adrenoreceptor agonists such as medetomidine by estrogen levels (Sinclair, 2003) and increased sensitivity to anesthesia with age (Friese et al., 2018). A previous work reported that 11 to 13-week-old female mice were more susceptible to isoflurane than male mice (Hohlbaum et al., 2017), consistent with the early death of females under anesthesia at 5 months of age in our study. At 14 months of age, our males exhibited a higher mortality than females. This effect was not related to any difficulties that might have been encountered in positioning larger male mice into the narrow space of the cryoprobe.

Adverse effects of isoflurane are dose dependent. Hypotension secondary to vasodilation may occur, as well as respiratory depression and gastrointestinal effects. However, the cardiodepressant effect is

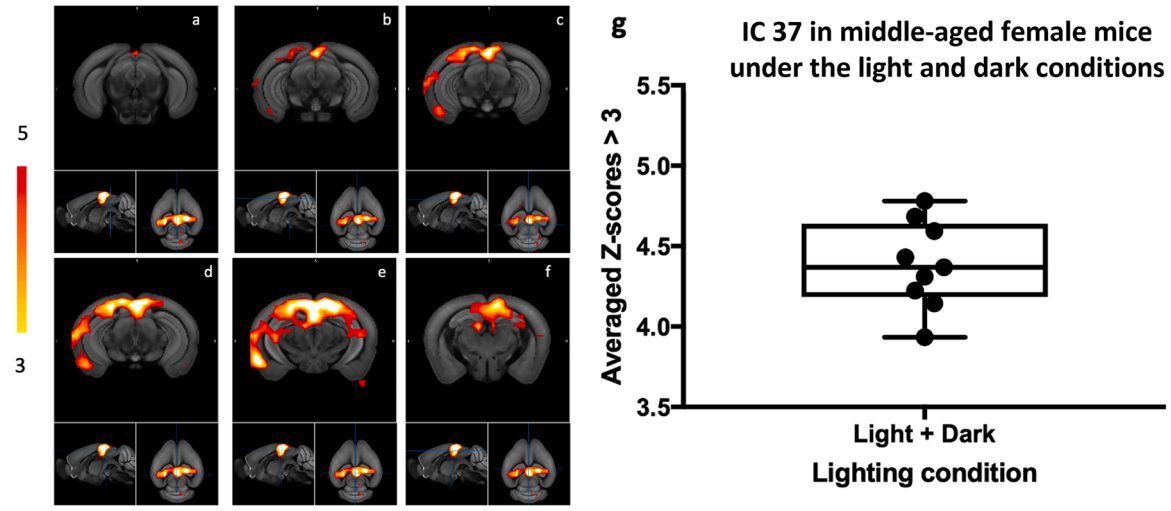

Fig. 4. Spatial maps of a plausible functional RSN-GICA (IC37) for which a significant difference between the light and dark conditions was found in middle-aged female mice. The network includes the retrosplenial cortex, pineal gland, and visual cortex. Z-scores are overlaid on the axial Allen Template image (with smaller orthogonal views) from caudal to rostral brain (a to f). The boxplot shows the averaged Z-score values of each middle-aged female mouse within the group (g). Z-scores were >3.

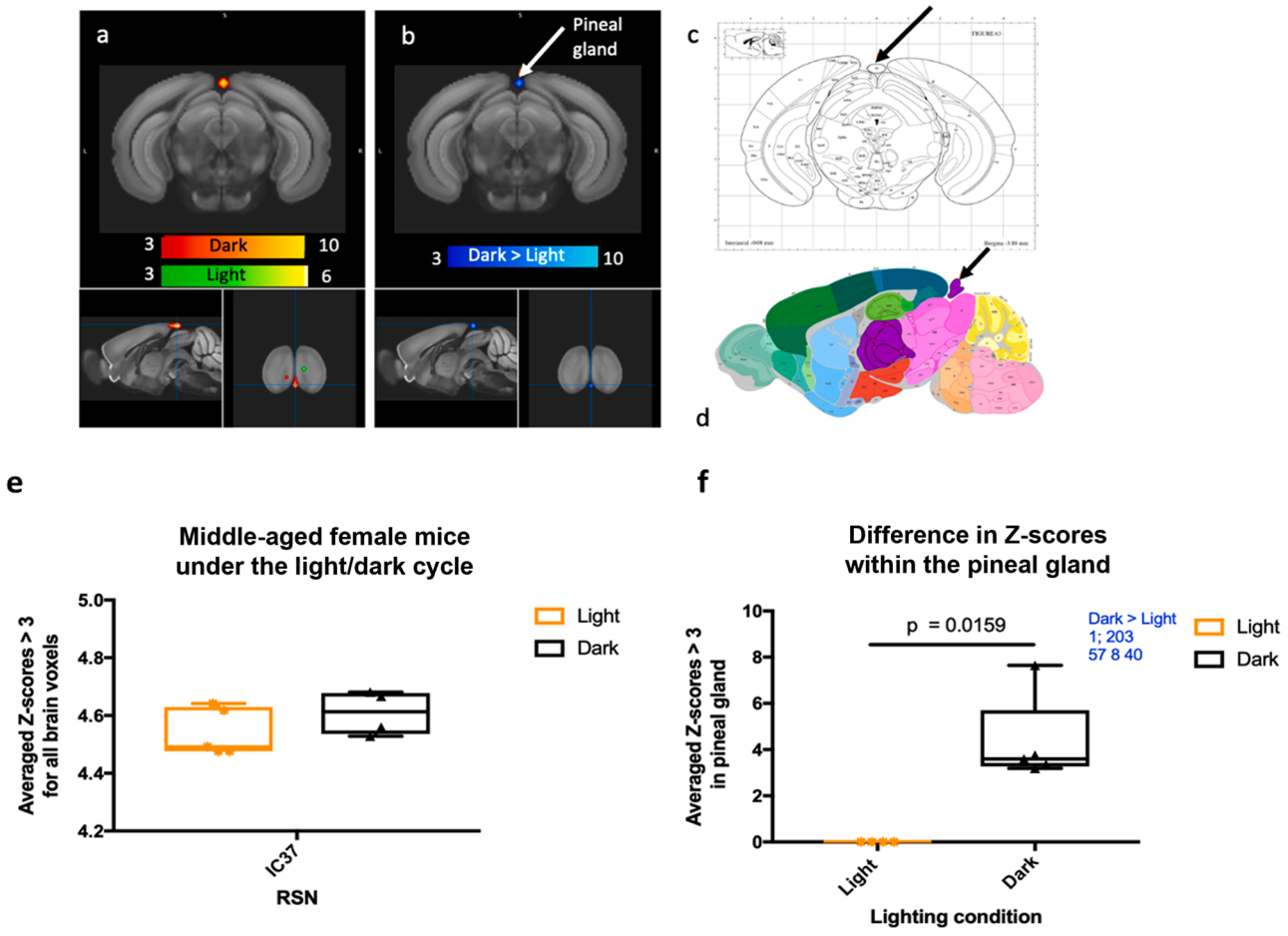

Fig. 5. Increased brain activity in the pineal gland of middle-aged female mice in the dark condition compared to the light condition. Spatial maps of clusters showing significant activation for IC37 under the light condition (green pixels) and the dark condition (red pixels) groups after DR and randomization test (a). A significant increase in FC was detected (blue cluster, arrows) in the dark condition compared to the light condition at the pineal gland (b) (see Paxinos (c) and Allen atlas (d)). Z-score color maps are overlaid on the Allen template (axial and smaller orthogonal views are shown). Averaged Z-scores values > 3 for all the voxels inside the component (e) and inside the cluster mask (f) are shown in the two groups. The cluster comprises 203 voxels with maximum intensity at 57 8 40 (x, y, z co-ordinates in the Allen Template).

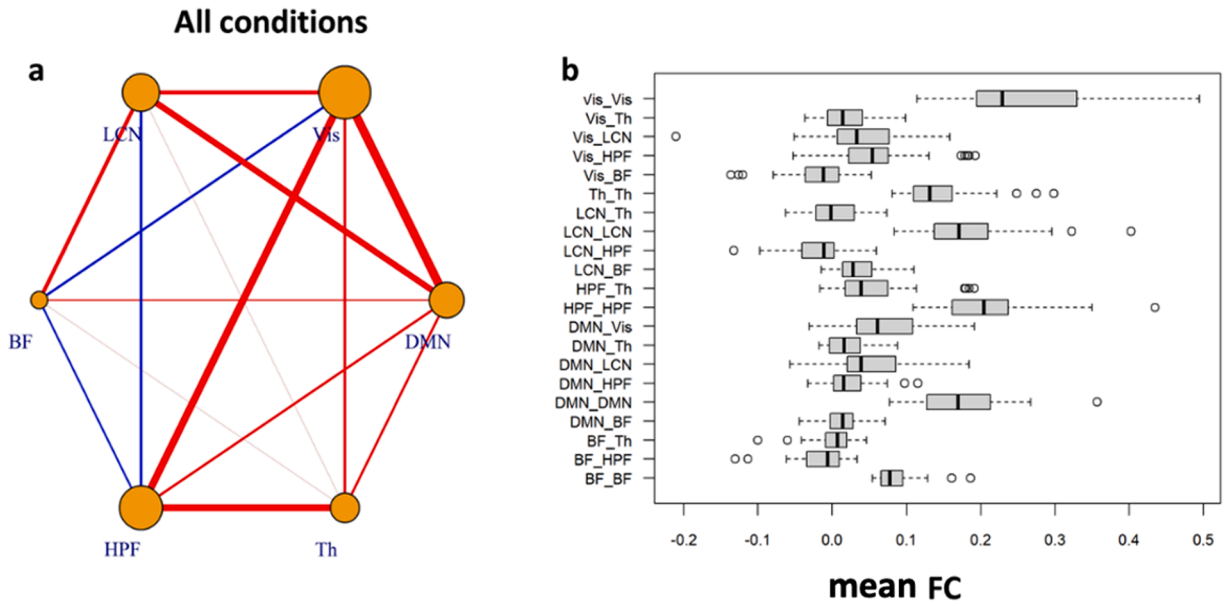

Fig. 6. Changes in FC across the RSNs derived from the literature independent of sex, age and lighting condition. Time series of BOLD signals averaged over voxels in RSN-LIT (orange circles in a) were used to calculate the Pearson correlation coefficients. Mean FC between each pair of networks was assessed in our sample (b) and presented as edges in a). Positive correlations are shown in red and negative correlations in blue. The thickness of the edges is proportional to the mean FC between two nodes, as are the areas of the different nodes which represent the mean FC between the subregions within each node. ***DMN**: Default Mode Network, **Vis**: Visual network, **LCN**: Lateral Cortical Network, **BF:** Basal Forebrain, **HPF:** Hippocampal Formation, **Th:** Thalamus.*

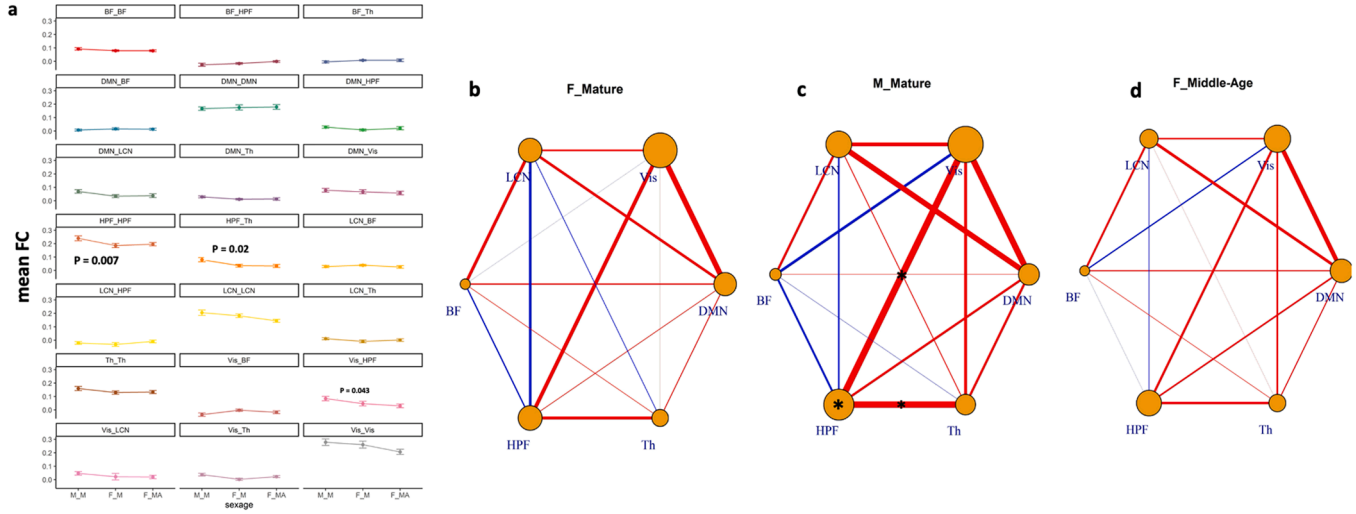

Fig. 7. Effects of sexage on FC of RSNs derived from the literature. Overall, FC was higher in mature male mice than in mature females, mainly affecting connections within HPF, and between Vis-HPF; HPF-Th (a-c). No significant difference in FC was observed as a function of age (a, b, and d). Positive correlations are shown in red and negative correlations in blue. The thickness of the edges is proportional to the mean FC between two nodes (orange circles), as are the areas of the different nodes which represent the mean FC between the subregions within each node. *Mature males (M_M) and middle-aged females (F_MA) were compared to mature females (F_M) (*p < 0.05 after correction for multiple comparisons). **DMN**: Default Mode Network, **Vis**: Visual network, **LCN**: Lateral Cortical Network, **BF:** Basal Forebrain, **HPF:** Hippocampal Formation, **Th:** Thalamus.*

generally minimal with this anesthetic (Plumb, 2008). A 6.5h-follow-up of 3 different strains of mice under isoflurane showed an unchanged heart rate for isoflurane concentrations up to 4 %, and a stable mean arterial blood pressure at concentrations below 2 %, which decreased for concentrations up to 4 % (Szczesny et al., 2004). In addition, rare adverse effects linked to the pharmacological properties of medetomidine have also been reported such as peripheral and cardiac vasoconstriction, bradycardia, decreased respiration, transient hypertension, hypothermia, urination, vomiting, hyperglycemia, prolonged sedation, hypersensitivity, pulmonary edema, apnea, and death from circulatory failure (Plumb, 2008). A 24h-follow-up of pregnant and non-pregnant rats after general anesthesia with a combination of medetomidine and ketamine led to the death of 15 % of the rats, irrespective of their pregnancy status suggesting airway obstruction (Callahan et al., 2014). In addition to respiratory issues, fluctuations in body temperature (hypo/hyperthermia) have also been reported under medetomidine, leading to the death of the animals (Callahan et al., 2014) and appearing linked to cardiac problems (Dugdale et al., 2010). These findings are consistent with our observations in two mice. Changes in gene expression after anesthesia have been found in most organs including the brain (Hamaya et al., 2000; Kotani et al., 1999; Paugam-Burtz et al., 2000) and probably depend on the type and duration of anesthesia (Kotani et al.,

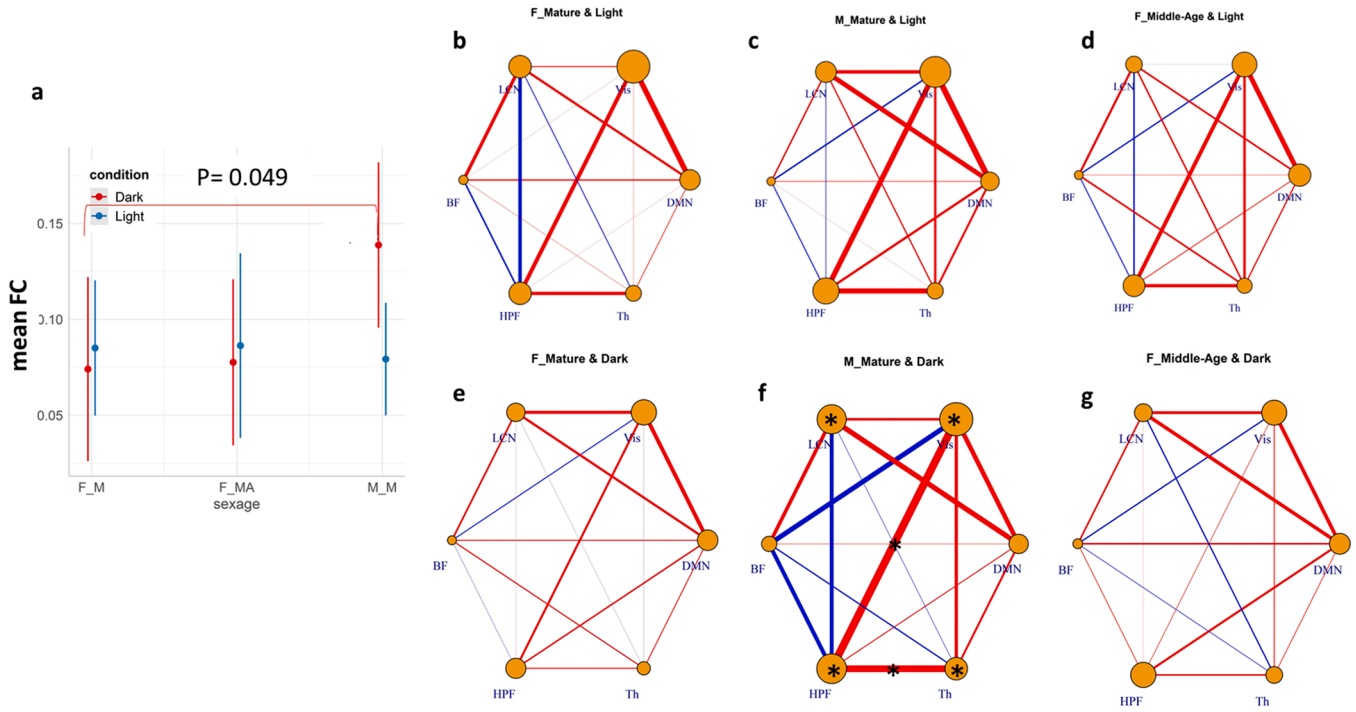

Fig. 8. Interaction effects of sexage and lighting condition on FC. Overall, FC was higher in mature male than in mature female mice under the dark condition (a). Despite the absence of significant interactions between sexage, lighting condition and edges, higher FC under the dark condition was found for connections within HPF, Th, Vis, LCN and Vis-HPF; HPF-Th **(e-f, asterisks)** in mature male mice compared to mature female mice. There were no significant differences under the light condition **(a, b-d)** or age **(a, e, and g)**. Positive correlations are shown in red and negative correlations in blue. The thickness of the edges is proportional to the mean FC between two nodes (orange circles), as are the areas of the different nodes which represent the mean FC between the subregions within each node. *Mature males (M_M) and middle-aged females (F_MA) were compared to mature females (F_M).* ***DMN:*** *Default Mode Network,* ***Vis:*** *Visual network,* ***LCN:*** *Lateral Cortical Network,* ***BF:*** *Basal Forebrain,* ***HPF:*** *Hippocampal Formation,* ***Th:*** *Thalamus.*

1999). In our study, mice were sedated and anesthetized 4 times over a 4-week period, both when they were mature and middle-aged. This repeated anesthetic regimen affects the expression of genes not only in the cardiorespiratory system but also in the brain and, combined with the increasing frailty in mice with ageing, made them more sensitive and vulnerable to anesthesia.

5. Limitations

One caveat of this study is that the animals' sleep was inevitably disrupted during the light condition (inactive phase) due to MRI explorations. We were also unable to perform a complete follow-up of all female and male mice due to increasing sensitivity to anesthesia (Friese et al., 2018) leading to motion or physiological instability and in some cases, to death. Moreover, the unpredictable occurrence of ulcerative dermatitis (Hampton et al., 2012; Sundberg et al., 2011) and fight wounds, as well as the predisposition to dysrhythmic breathing with ageing (Stettner et al., 2008; Yamauchi et al., 2010), reduced the number of usable data, particularly for male mice. However, the group size was sufficient to study the main effects of sex and lighting condition as well as their interaction on RSNs but not to assess the effect of age. Consequently, the effects of light/dark alternation on RSNs in middle-aged mice were examined only in females. The absence of a significant interaction when considering edges, sexage and lighting condition simultaneously could reflect insufficient statistical power. Although we studied the effect of day/night alternation on brain connectivity, we did not investigate the impact of circadian rhythms, which would have required additional light regimes (eg constant light and constant darkness) and monitoring rhythmicity of locomotor activity under the different conditions, a behavioral outcome used as a read-out for circadian rhythms.

6. Conclusion

The present work shows changes in brain activity as a function of lighting condition in the pineal gland in middle-aged females. We also detected sex-differences in brain activity in cortical, hippocampal and midbrain regions in mature mice independent of lighting condition. Interestingly, we observed a sex difference in network laterality with bilateral functional networks systematically present in males that was confirmed by seed-based analysis. Region-level analyses showed that FC is influenced by the interaction between i) sexage and edges and ii) sexage and day/night cycle. This pilot study highlights the importance of considering the adverse effects of repeated anesthesia related to age and biological sex by increasing the group size for longitudinal studies.

Funding

This work was funded by the French National Research Agency ANR "Connectome" (grant ANR-17-CE37-0001-03) and France Alzheimer-APP-PFA2020-BERNARD. CRMBM is a member of France Life Imaging (grant ANR-11-370 INBS-0006 from the French "Investissements d'Avenir" program).

CRediT authorship contribution statement

Houéfa Armelle Lokossou: Writing – review & editing, Writing – original draft, Project administration, Methodology, Investigation, Formal analysis. **Giovanni Rabuffo:** Writing – review & editing, Methodology. **Monique Bernard:** Funding acquisition. **Christophe Bernard:** Writing – review & editing, Conceptualization. **Angèle Viola:** Writing – review & editing, Validation, Supervision, Resources, Funding acquisition, Conceptualization. **Teodora-Adriana Perles-Barbacaru:** Writing – review & editing, Validation, Supervision, Conceptualization.

Declaration of competing interest

None.

Data availability

Data will be made available on request.

Acknowledgments

We gratefully acknowledge M. Bernard Giusiano for his help with the statistical methodology.

Supplementary materials

Supplementary material associated with this article can be found, in the online version, at doi:10.1016/j.neuroimage.2024.120576.

References

Angel, A., 1993. Central neuronal pathways and the process of anesthesia. Br. J. Anaesth. 71, 148–163. https://doi.org/10.1093/bja/71.1.148.

Arendt, J., Skene, D.J., 2005. Melatonin as a chronobiotic. Sleep Med. Rev. 9, 25–39. https://doi.org/10.1016/j.smrv.2004.05.002.

Bailey, M., Silver, R., 2014. Sex differences in circadian timing systems: implications for disease. Front. Neuroendocrinol. 35, 111–139. https://doi.org/10.1016/j.yfrne.2013.11.003.

Bajic, D., Craig, M.M., Mongerson, C.R.L., Borsook, D., Becerra, L., 2017. Identifying rodent resting-state brain networks with independent component analysis. Front. Neurosci. 11, 685. https://doi.org/10.3389/fnins.2017.00685.

Bartoň, M., Mareček, R., Krajčovičová, L., Slavíček, T., Kašpárek, T., Zemánková, P., Říha, P., Mikl, M., 2019. Evaluation of different cerebrospinal fluid and white matter fMRI filtering strategies-quantifying noise removal and neural signal preservation. Hum. Brain Mapp. 40, 1114–1138. https://doi.org/10.1002/hbm.24433.

Beckmann, C.F., Smith, S.M., 2004. Probabilistic independent component analysis for functional magnetic resonance imaging. IEEE Trans. Med. Imaging 23, 137–152. https://doi.org/10.1109/TMI.2003.822821.

Bell, P.T., Shine, J.M., 2016. Subcortical contributions to large-scale network communication. Neurosci. Biobehav. Rev. 71, 313–322. https://doi.org/10.1016/j.neubiorev.2016.08.036.

Bernard, C., 2021. Circadian/multidien molecular oscillations and rhythmicity of epilepsy (MORE). Epilepsia 62 (Suppl 1), S49–S68. https://doi.org/10.1111/epi.16716.

Birn, R.M., 2012. The role of physiological noise in resting-state functional connectivity. Neuroimage 62, 864–870. https://doi.org/10.1016/j.neuroimage.2012.01.016.

Biswal, B., Yetkin, F.Z., Haughton, V.M., Hyde, J.S., 1995. Functional connectivity in the motor cortex of resting human brain using echo-planar MRI. Magn. Reson. Med. 34, 537–541. https://doi.org/10.1002/mrm.1910340409.

Biswal, B.B., Mennes, M., Zuo, X.-N., Gohel, S., Kelly, C., Smith, S.M., Beckmann, C.F., Adelstein, J.S., Buckner, R.L., Colcombe, S., Dogonowski, A.-M., Ernst, M., Fair, D., Hampson, M., Hoptman, M.J., Hyde, J.S., Kiviniemi, V.J., Kötter, R., Li, S.-J., Lin, C.-P., Lowe, M.J., Mackay, C., Madden, D.J., Madsen, K.H., Margulies, D.S., Mayberg, H.S., McMahon, K., Monk, C.S., Mostofsky, S.H., Nagel, B.J., Pekar, J.J., Peltier, S.J., Petersen, S.E., Riedl, V., Rombouts, S.A.R.B., Rypma, B., Schlaggar, B.L., Schmidt, S., Seidler, R.D., Siegle, G.J., Sorg, C., Teng, G.-J., Veijola, J., Villringer, A., Walter, M., Wang, L., Weng, X.-C., Whitfield-Gabrieli, S., Williamson, P., Windischberger, C., Zang, Y.-F., Zhang, H.-Y., Castellanos, F.X., Milham, M.P., 2010. Toward discovery science of human brain function. Proc. Natl. Acad. Sci 107, 4734–4739. https://doi.org/10.1073/pnas.0911855107.

Blautzik, J., Vetter, C., Schneider, A., Gutyrchik, E., Reinisch, V., Keeser, D., Paolini, M., Pöppel, E., Bao, Y., Reiser, M., Roenneberg, T., Meindl, T., 2014. Dysregulated daily rhythmicity of neuronal resting-state networks in MCI patients. Chronobiol. Int. 31, 1041–1050. https://doi.org/10.3109/07420528.2014.944618.

Boveroux, P., Vanhaudenhuyse, A., Bruno, M.-A., Noirhomme, Q., Lauwick, S., Luxen, A., Degueldre, C., Plenevaux, A., Schnakers, C., Phillips, C., Brichant, J.-F., Bonhomme, V., Maquet, P., Greicius, M.D., Laureys, S., Boly, M., 2010. Breakdown of within- and between-network resting state functional magnetic resonance imaging connectivity during propofol-induced loss of consciousness. Anesthesiology 113, 1038–1053. https://doi.org/10.1097/ALN.0b013e3181f697f5.

Brown, E.N., Lydic, R., Schiff, N.D., 2010. General anesthesia, sleep, and coma. N. Engl. J. Med. 363, 2638–2650. https://doi.org/10.1056/NEJMra0808281.

Bukhari, Q., Schroeter, A., Cole, D.M., Rudin, M., 2017. Resting state fMRI in mice reveals anesthesia specific signatures of brain functional networks and their interactions. Front. Neur. Circuit. 11 https://doi.org/10.3389/fncir.2017.00005.

Callahan, L.M., Ross, S.M., Jones, M.L., Musk, G.C., 2014. Mortality associated with using medetomidine and ketamine for general anesthesia in pregnant and nonpregnant Wistar rats. Lab. Anim. 43, 208–214. https://doi.org/10.1038/laban.517.

Campagna, J.A., Miller, K.W., Forman, S.A., 2003. Mechanisms of actions of inhaled anesthetics. N. Engl. J. Med. 348, 2110–2124. https://doi.org/10.1056/NEJMra021261.

Campagner, D., Vale, R., Tan, Y.L., Iordanidou, P., Pavón Arocas, O., Claudi, F., Stempel, A.V., Keshavarzi, S., Petersen, R.S., Margrie, T.W., Branco, T., 2023. A cortico-collicular circuit for orienting to shelter during escape. Nature 613, 111–119. https://doi.org/10.1038/s41586-022-05553-9.

Canto, C.B., Onuki, Y., Bruinsma, B., van der Werf, Y.D., De Zeeuw, C.I., 2017. The sleeping cerebellum. Trend. Neurosci. 40, 309–323. https://doi.org/10.1016/j.tins.2017.03.001.

Chen, C.S., Ebitz, R.B., Bindas, S.R., Redish, A.D., Hayden, B.Y., Grissom, N.M., 2021. Divergent strategies for learning in males and females. Curr. Biol. CB 31. https://doi.org/10.1016/j.cub.2020.09.075, 39-50.e4.

Colon, L.M., Poulos, A.M., 2020. Contextual processing elicits sex differences in dorsal hippocampus activation following footshock and context fear retrieval. Behav. Brain Res. 393, 112771 https://doi.org/10.1016/j.bbr.2020.112771.

Conti, A., Maestroni, G.J., 1996. HPLC validation of a circadian melatonin rhythm in the pineal gland of inbred mice. J. Pineal Res. 20, 138–144. https://doi.org/10.1111/j.1600-079x.1996.tb00249.x.

Cooper, B.G., Mizumori, S.J., 2001. Temporary inactivation of the retrosplenial cortex causes a transient reorganization of spatial coding in the hippocampus. J. Neurosci. Off. J. Soc. Neurosci. 21, 3986–4001. https://doi.org/10.1523/JNEUROSCI.21-11-03986.2001.

Daneault, V., Orban, P., Martin, N., Dansereau, C., Godbout, J., Pouliot, P., Dickinson, P., Gosselin, N., Vandewalle, G., Maquet, P., Lina, J.-M., Doyon, J., Bellec, P., Carrier, J., 2021. Cerebral functional networks during sleep in young and older individuals. Sci. Rep. 11, 4905. https://doi.org/10.1038/s41598-021-84417-0.

De Zeeuw, C.I., Ten Brinke, M.M., 2015. Motor learning and the cerebellum. Cold Spring Harb. Perspect. Biol. 7, a021683 https://doi.org/10.1101/cshperspect.a021683.

Duffy, J.F., Zitting, K.-M., Chinoy, E.D., 2015. Aging and circadian rhythms. Sleep Med. Clin. 10, 423–434. https://doi.org/10.1016/j.jsmc.2015.08.002.

Dugdale, A., Beaumont, G., Bradbrook, C., Gurney, M., 2010. Veterinary Anaesthesia: Principles to Practice, 2nd Edition. Wiley.com. URL. https://www.wiley.com/en-us/Veterinary+Anaesthesia%3A+Principles+to+Practice%2C+2nd+Edition-p-9781119246770. (accessed 3.6.23).

Dutta, S., Sengupta, P., 2016. Men and mice: relating their ages. Life Sci. 152, 244–248. https://doi.org/10.1016/j.lfs.2015.10.025.

Ebihara, S., Marks, T., Hudson, D.J., Menaker, M., 1986. Genetic control of melatonin synthesis in the pineal gland of the mouse. Science 231, 491–493. https://doi.org/10.1126/science.3941912.

Fafrowicz, M., Bohaterewicz, B., Ceglarek, A., Cichocka, M., Lewandowska, K., Sikora-Wachowicz, B., Oginska, H., Beres, A., Olszewska, J., Marek, T., 2019. Beyond the low frequency fluctuations: morning and evening differences in human brain. Front. Hum. Neurosci. 13, 288. https://doi.org/10.3389/fnhum.2019.00288.

Farahani, F.V., Karwowski, W., D'Esposito, M., Betzel, R.F., Douglas, P.K., Sobczak, A.M., Bohaterewicz, B., Marek, T., Fafrowicz, M., 2022. Diurnal variations of resting-state fMRI data: a graph-based analysis. Neuroimage 256, 119246. https://doi.org/10.1016/j.neuroimage.2022.119246.

Farahani, V.F., Fafrowicz, M., Karwowski, W., Bohaterewicz, B., Sobczak, A.M., Ceglarek, A., Zyrkowska, A., Ostrogorska, M., Sikora-Wachowicz, B., Lewandowska, K., Oginska, H., Beres, A., Hubalewska-Mazgaj, M., Marek, T., 2021. Identifying diurnal variability of brain connectivity patterns using graph theory. Brain Sci. 11, 111. https://doi.org/10.3390/brainsci11010111.

Filippini, N., MacIntosh, B.J., Hough, M.G., Goodwin, G.M., Frisoni, G.B., Smith, S.M., Matthews, P.M., Beckmann, C.F., Mackay, C.E., 2009. Distinct patterns of brain activity in young carriers of the *APOE* -ε4 allele. Proc. Natl. Acad. Sci 106, 7209–7214. https://doi.org/10.1073/pnas.0811879106.

Fox, M.D., Raichle, M.E., 2007. Spontaneous fluctuations in brain activity observed with functional magnetic resonance imaging. Nat. Rev. Neurosci. 8, 700–711. https://doi.org/10.1038/nrn2201.

Friese, M.B., Nathan, M., Culley, D.J., Crosby, G., 2018. Isoflurane anesthesia impairs the expression of immune neuromodulators in the hippocampus of aged mice. PLoS ONE 13, e0209283. https://doi.org/10.1371/journal.pone.0209283.

Gawryluk, J.R., Mazerolle, E.L., D'Arcy, R.C.N., 2014. Does functional MRI detect activation in white matter? A review of emerging evidence, issues, and future directions. Front. Neurosci. 8 https://doi.org/10.3389/fnins.2014.00239.

Gökmen, N., Barış, İ., Öçmen, E., Yılmaz, O., Günerli, A., Kavaklı, İ.H., 2017. Day-time isoflurane administration suppresses circadian gene expressions in both the brain and a peripheral organ. Liver. Turk. J. Anaesthesiol. Reanim. 45, 197–202. https://doi.org/10.5152/TJAR.2017.68466.

Goto, M., Oshima, I., Tomita, T., Ebihara, S., 1989. Melatonin content of the pineal gland in different mouse strains. J. Pineal Res. 7, 195–204. https://doi.org/10.1111/j.1600-079x.1989.tb00667.x.

Grandjean, J., Canella, C., Anckaerts, C., Ayrancı, G., Bougacha, S., Bienert, T., Buehlmann, D., Coletta, L., Gallino, D., Gass, N., Garin, C.M., Nadkarni, N.A., Hübner, N.S., Karatas, M., Komaki, Y., Kreitz, S., Mandino, F., Mechling, A.E., Sato, C., Sauer, K., Shah, D., Strobelt, S., Takata, N., Wank, I., Wu, T., Yahata, N., Yeow, L.Y., Yee, Y., Aoki, I., Chakravarty, M.M., Chang, W.-T., Dhenain, M., von Elverfeldt, D., Harsan, L.-A., Hess, A., Jiang, T., Keliris, G.A., Lerch, J.P., Meyer-Lindenberg, A., Okano, H., Rudin, M., Sartorius, A., Van der Linden, A., Verhoye, M., Weber-Fahr, W., Wenderoth, N., Zerbi, V., Gozzi, A., 2020. Common functional networks in the mouse brain revealed by multi-centre resting-state fMRI analysis. Neuroimage 205, 116278. https://doi.org/10.1016/j.neuroimage.2019.116278.

Grandjean, J., Schroeter, A., Batata, I., Rudin, M., 2014. Optimization of anesthesia protocol for resting-state fMRI in mice based on differential effects of anesthetics on

functional connectivity patterns. Neuroimage 102, 838–847. https://doi.org/10.1016/j.neuroimage.2014.08.043.
Greicius, M.D., Kiviniemi, V., Tervonen, O., Vainionpää, V., Alahuhta, S., Reiss, A.L., Menon, V., 2008. Persistent default-mode network connectivity during light sedation. Hum. Brain Mapp. 29, 839–847. https://doi.org/10.1002/hbm.20537.
Guilding, C., Piggins, H.D., 2007. Challenging the omnipotence of the suprachiasmatic timekeeper: are circadian oscillators present throughout the mammalian brain?: circadian oscillators in mammalian brain. Eur. J. Neurosci. 25, 3195–3216. https://doi.org/10.1111/j.1460-9568.2007.05581.x.
Guldenmund, P., Demertzi, A., Boveroux, P., Boly, M., Vanhaudenhuyse, A., Bruno, M.-A., Gosseries, O., Noirhomme, Q., Brichant, J.-F., Bonhomme, V., Laureys, S., Soddu, A., 2013. Thalamus, Brainstem and Salience Network Connectivity Changes During Propofol-Induced Sedation and Unconsciousness. Brain Connect. 3, 273–285. https://doi.org/10.1089/brain.2012.0117.
Guldenmund, P., Vanhaudenhuyse, A., Sanders, R.D., Sleigh, J., Bruno, M.A., Demertzi, A., Bahri, M.A., Jaquet, O., Sanfilippo, J., Baquero, K., Boly, M., Brichant, J.F., Laureys, S., Bonhomme, V., 2017. Brain functional connectivity differentiates dexmedetomidine from propofol and natural sleep. Br. J. Anaesth. 119, 674–684. https://doi.org/10.1093/bja/aex257.
Hagan, C., 2017. When are mice considered old? Jackson Lab. URL https://www.jax.org/news-and-insights/jax-blog/2017/November/when-are-mice-considered-old (accessed 11.2.22).
Hamaya, Y., Takeda, T., Dohi, S., Nakashima, S., Nozawa, Y., 2000. The effects of pentobarbital, isoflurane, and propofol on immediate-early gene expression in the vital organs of the rat. Anesth. Analg. 90, 1177–1183. https://doi.org/10.1097/00000539-200005000-00034.
Hampton, A.L., Hish, G.A., Aslam, M.N., Rothman, E.D., Bergin, I.L., Patterson, K.A., Naik, M., Paruchuri, T., Varani, J., Rush, H.G., 2012. Progression of ulcerative dermatitis lesions in C57BL/6Crl mice and the development of a scoring system for dermatitis lesions. J. Am. Assoc. Lab. Anim. Sci. JAALAS 51, 586.
Harris, S.S., Boorman, L.W., Das, D., Kennerley, A.J., Sharp, P.S., Martin, C., Redgrave, P., Schwartz, T.H., Berwick, J., 2018. Physiological and pathological brain activation in the anesthetized rat produces hemodynamic-dependent cortical temperature increases that can confound the BOLD fMRI signal. Front. Neurosci. 12.
Heine, L., Soddu, A., Gomez, F., Vanhaudenhuyse, A., Tshibanda, L., Thonnard, M., Charland-Verville, V., Kirsch, M., Laureys, S., Demertzi, A., 2012. Resting state networks and consciousness. Front. Psychol. 3.
Hohlbaum, K., Bert, B., Dietze, S., Palme, R., Fink, H., Thöne-Reineke, C., 2017. Severity classification of repeated isoflurane anesthesia in C57BL/6JRj mice—Assessing the degree of distress. PLoS ONE 12, e0179588. https://doi.org/10.1371/journal.pone.0179588.
Jenkinson, M., Bannister, P., Brady, M., Smith, S., 2002a. Improved optimization for the robust and accurate linear registration and motion correction of brain images. Neuroimage 17, 825–841. https://doi.org/10.1006/nimg.2002.1132.
Jenkinson, M., Bannister, P., Brady, M., Smith, S., 2002b. Improved optimization for the robust and accurate linear registration and motion correction of brain images. Neuroimage 17, 825–841. https://doi.org/10.1016/s1053-8119(02)91132-8.
Jordan, D., Ilg, R., Riedl, V., Schorer, A., Grimberg, S., Neufang, S., Omerovic, A., Berger, S., Untergehrer, G., Preibisch, C., Schulz, E., Schuster, T., Schröter, M., Spoormaker, V., Zimmer, C., Hemmer, B., Wohlschläger, A., Kochs, E.F., Schneider, G., 2013. Simultaneous electroencephalographic and functional magnetic resonance imaging indicate impaired cortical top–down processing in association with anesthetic-induced unconsciousness. Anesthesiology 119, 1031–1042. https://doi.org/10.1097/ALN.0b013e3182a7ca92.
Kalmbach, A.S., Waters, J., 2012. Brain surface temperature under a craniotomy. J. Neurophysiol. 108, 3138–3146. https://doi.org/10.1152/jn.00557.2012.
Kasahara, T., Abe, K., Mekada, K., Yoshiki, A., Kato, T., 2010. Genetic variation of melatonin productivity in laboratory mice under domestication. Proc. Natl. Acad. Sci. 107, 6412–6417. https://doi.org/10.1073/pnas.0914399107.
Keene, C.S., Bucci, D.J., 2008. Contributions of the retrosplenial and posterior parietal cortices to cue-specific and contextual fear conditioning. Behav. Neurosci. 122, 89–97. https://doi.org/10.1037/0735-7044.122.1.89.
Kotani, N., Hashimoto, H., Sessler, D.I., Yasuda, T., Ebina, T., Muraoka, M., Matsuki, A., 1999. Expression of genes for proinflammatory cytokines in alveolar macrophages during propofol and isoflurane anesthesia. Anesth. Analg. 89, 1250–1256.
Langevad, L., Madsen, C.G., Siebner, H., Garde, E., 2014. [MRI of the pineal gland]. Ugeskr. Laeger 176, V07140395.
Larson-Prior, L.J., Zempel, J.M., Nolan, T.S., Prior, F.W., Snyder, A.Z., Raichle, M.E., 2009. Cortical network functional connectivity in the descent to sleep. Proc. Natl. Acad. Sci. 106, 4489–4494. https://doi.org/10.1073/pnas.0900924106.
Li, Y., Wang, S., Pan, C., Xue, F., Xian, J., Huang, Y., Wang, X., Li, T., He, H., 2018. Comparison of NREM sleep and intravenous sedation through local information processing and whole brain network to explore the mechanism of general anesthesia. PLoS ONE 13, e0192358. https://doi.org/10.1371/journal.pone.0192358.
Liska, A., Galbusera, A., Schwarz, A.J., Gozzi, A., 2015. Functional connectivity hubs of the mouse brain. Neuroimage 115, 281–291. https://doi.org/10.1016/j.neuroimage.2015.04.033.
Macchi, M.M., Bruce, J.N., 2004. Human pineal physiology and functional significance of melatonin. Front. Neuroendocrinol. 25, 177–195. https://doi.org/10.1016/j.yfrne.2004.08.001.
Mähler Convenor, M., Berard, M., Feinstein, R., Gallagher, A., Illgen-Wilcke, B., Pritchett-Corning, K., Raspa, M., 2014. FELASA recommendations for the health monitoring of mouse, rat, hamster, guinea pig and rabbit colonies in breeding and experimental units. Lab. Anim. 48, 178–192. https://doi.org/10.1177/0023677213516312.
Mandino, F., Vrooman, R.M., Foo, H.E., Yeow, L.Y., Bolton, T.A.W., Salvan, P., Teoh, C. L., Lee, C.Y., Beauchamp, A., Luo, S., Bi, R., Zhang, J., Lim, G.H.T., Low, N., Sallet, J., Gigg, J., Lerch, J.P., Mars, R.B., Olivo, M., Fu, Y., Grandjean, J., 2022. A triple-network organization for the mouse brain. Mol. Psychiatry 27, 865–872. https://doi.org/10.1038/s41380-021-01298-5.
Manukian, K.H., Kirakosian, L.G., 1985. Proteolipids in developing rat brain. Neurochem. Res. 10, 1533–1545.
McCauley, J.P., Petroccione, M.A., D'Brant, L.Y., Todd, G.C., Affinnih, N., Wisnoski, J.J., Zahid, S., Shree, S., Sousa, A.A., De Guzman, R.M., Migliore, R., Brazhe, A., Leapman, R.D., Khmaladze, A., Semyanov, A., Zuloaga, D.G., Migliore, M., Scimemi, A., 2020. Circadian modulation of neurons and astrocytes controls synaptic plasticity in hippocampal area CA1. Cell Rep. 33, 108255 https://doi.org/10.1016/j.celrep.2020.108255.
Melozzi, F., Bergmann, E., Harris, J.A., Kahn, I., Jirsa, V., Bernard, C., 2019. Individual structural features constrain the mouse functional connectome. Proc. Natl. Acad. Sci. U. S. A., 201906694 https://doi.org/10.1073/pnas.1906694116.
Melozzi, F., Woodman, M.M., Jirsa, V.K., Bernard, C., 2017. The virtual mouse brain: a computational neuroinformatics platform to study whole mouse brain dynamics. eNeuro 4. https://doi.org/10.1523/ENEURO.0111-17.2017. ENEURO.0111-17.2017.
Moon, E., Kim, K., Partonen, T., Linnaranta, O., 2022. Role of melatonin in the management of sleep and circadian disorders in the context of psychiatric illness. Curr. Psychiatry Rep. 24, 623–634. https://doi.org/10.1007/s11920-022-01369-6.
Murakami, T., Ohki, K., 2023. Thalamocortical circuits for the formation of hierarchical pathways in the mammalian visual cortex. Front. Neural Circuits 17, 1155195. https://doi.org/10.3389/fncir.2023.1155195.
Murphy, K., Birn, R.M., Handwerker, D.A., Jones, T.B., Bandettini, P.A., 2009. The impact of global signal regression on resting state correlations: are anti-correlated networks introduced? Neuroimage 44, 893–905. https://doi.org/10.1016/j.neuroimage.2008.09.036.
Murphy, M., Bruno, M.-A., Riedner, B.A., Boveroux, P., Noirhomme, Q., Landsness, E.C., Brichant, J.-F., Phillips, C., Massimini, M., Laureys, S., Tononi, G., Boly, M., 2011. Propofol anesthesia and sleep: a high-density EEG study. Sleep 34, 283–291A. https://doi.org/10.1093/sleep/34.3.283.
Nakamura, K., Brown, R.A., Narayanan, S., Collins, D.L., Arnold, D.L., Alzheimer's Disease Neuroimaging Initiative, 2015. Diurnal fluctuations in brain volume: statistical analyses of MRI from large populations. Neuroimage 118, 126–132. https://doi.org/10.1016/j.neuroimage.2015.05.077.
Neag, M.-A., Mitre, A.-O., Catinean, A., Mitre, C.-I., 2020. An overview on the mechanisms of neuroprotection and neurotoxicity of isoflurane and sevoflurane in experimental studies. Brain Res. Bull. 165, 281–289. https://doi.org/10.1016/j.brainresbull.2020.10.011.
Nelson, J.F., Felicio, L.S., Randall, P.K., Sims, C., Finch, C.E., 1982. A longitudinal study of estrous cyclicity in aging C57BL/6J mice: I. Cycle frequency, length and vaginal cytology1. Biol. Reprod. 27, 327–339. https://doi.org/10.1095/biolreprod27.2.327.
Nichols, T.E., Holmes, A.P., 2002. Nonparametric permutation tests for functional neuroimaging: a primer with examples. Hum. Brain Mapp. 15, 1–25. https://doi.org/10.1002/hbm.1058.
Nickerson, L.D., Smith, S.M., Öngür, D., Beckmann, C.F., 2017. Using dual regression to investigate network shape and amplitude in functional connectivity analyses. Front. Neurosci. 11 https://doi.org/10.3389/fnins.2017.00115.
Nir, T., Raizman, R., Meningher, I., Jacob, Y., Huang, K.-H., Schwartz, A.E., Brallier, J. W., Ahn, H., Kundu, P., Tang, C.Y., Delman, B.N., McCormick, P.J., Scarpa, J., Sano, M., Deiner, S.G., Livny, A., Baxter, M.G., Mincer, J.S., 2022. Lateralisation of subcortical functional connectivity during and after general anaesthesia. Br. J. Anaesth. 128, 65–76. https://doi.org/10.1016/j.bja.2021.08.033.
Okatani, Y., Morioka, N., Hayashi, K., 1999. Changes in nocturnal pineal melatonin synthesis during the perimenopausal period: relation to estrogen levels in female rats. J. Pineal Res. 27, 65–72. https://doi.org/10.1111/j.1600-079X.1999.tb00598.x.
Okatani, Y., Morioka, N., Wakatsuki, A., 2000. Changes in nocturnal melatonin secretion in perimenopausal women: correlation with endogenous estrogen concentrations. J. Pineal Res. 28, 111–118. https://doi.org/10.1034/j.1600-079X.2001.280207.x.
Orban, C., Kong, R., Li, J., Chee, M.W.L., Yeo, B.T.T., 2021. Correction: time of day is associated with paradoxical reductions in global signal fluctuation and functional connectivity. PLoS Biol. 19, e3001258 https://doi.org/10.1371/journal.pbio.3001258.
Paugam-Burtz, C., Molliex, S., Lardeux, B., Rolland, C., Aubier, M., Desmonts, J.M., Crestani, B., 2000. Differential effects of halothane and thiopental on surfactant protein C messenger RNA in vivo and in vitro in rats. Anesthesiology 93, 805–810. https://doi.org/10.1097/00000542-200009000-00030.
Percie du Sert, N., Ahluwalia, A., Alam, S., Avey, M.T., Baker, M., Browne, W.J., Clark, A., Cuthill, I.C., Dirnagl, U., Emerson, M., Garner, P., Holgate, S.T., Howells, D.W., Hurst, V., Karp, N.A., Lazic, S.E., Lidster, K., MacCallum, C.J., Macleod, M., Pearl, E.J., Petersen, O.H., Rawle, F., Reynolds, P., Rooney, K., Sena, E. S., Silberberg, S.D., Steckler, T., Würbel, H., 2020. Reporting animal research: explanation and elaboration for the ARRIVE guidelines 2.0. PLOS Biol. 18, e3000411 https://doi.org/10.1371/journal.pbio.3000411.
Pierce, J.E., Thomasson, M., Voruz, P., Selosse, G., Péron, J., 2023. Explicit and implicit emotion processing in the cerebellum: a meta-analysis and systematic review. Cerebellum Lond. Engl. 22, 852–864. https://doi.org/10.1007/s12311-022-01459-4.
Pierpaoli, W., Regelson, W., 1994. Pineal control of aging: effect of melatonin and pineal grafting on aging mice. Proc. Natl. Acad. Sci. U. S. A. 91, 787–791.

Pletzer, B., Harris, T., 2018. Sex hormones modulate the relationship between global advantage, lateralization, and interhemispheric connectivity in a Navon paradigm. Brain Connect. 8, 106–118. https://doi.org/10.1089/brain.2017.0504.

Plumb, D.C., 2008. Plumb's veterinary drug handbook sixth edition. Vet. Pathol. 45, 1136. https://doi.org/10.1354/vp.45-6-952-a.

Poulsen, R.C., Warman, G.R., Sleigh, J., Ludin, N.M., Cheeseman, J.F., 2018. How does general anaesthesia affect the circadian clock? Sleep Med. Rev. 37, 35–44. https://doi.org/10.1016/j.smrv.2016.12.002.

Powell, A., Connelly, W.M., Vasalauskaite, A., Nelson, A.J.D., Vann, S.D., Aggleton, J.P., Sengpiel, F., Ranson, A., 2020. Stable encoding of visual cues in the mouse retrosplenial cortex. Cereb. Cortex 30, 4424–4437. https://doi.org/10.1093/cercor/bhaa030.

Power, J.D., Barnes, K.A., Snyder, A.Z., Schlaggar, B.L., Petersen, S.E., 2012. Spurious but systematic correlations in functional connectivity MRI networks arise from subject motion. Neuroimage 59, 2142–2154. https://doi.org/10.1016/j.neuroimage.2011.10.018.

Purdon, P.L., Pierce, E.T., Bonmassar, G., Walsh, J., Harrell, P.G., Kwo, J., Deschler, D., Barlow, M., Merhar, R.C., Lamus, C., Mullaly, C.M., Sullivan, M., Maginnis, S., Skoniecki, D., Higgins, H.-A., Brown, E.N., 2009. Simultaneous electroencephalography and functional magnetic resonance imaging of general anesthesia. Ann. N.Y. Acad. Sci. 1157, 61–70. https://doi.org/10.1111/j.1749-6632.2008.04119.x.

Roy, D.S., Zhang, Y., Halassa, M.M., Feng, G., 2022. Thalamic subnetworks as units of function. Nat. Neurosci. 25, 140–153. https://doi.org/10.1038/s41593-021-00996-1.

Sapède, D., Cau, E., 2013. The pineal gland from development to function. Current Topics in Developmental Biology 171–215. https://doi.org/10.1016/B978-0-12-416021-7.00005-5.

Schlichting, M.L., Zeithamova, D., Preston, A.R., 2014. CA1 subfield contributions to memory integration and inference. Hippocampus 24, 1248–1260. https://doi.org/10.1002/hipo.22310.

Sinclair, M.D., 2003. A review of the physiological effects of alpha2-agonists related to the clinical use of medetomidine in small animal practice. Can. Vet. J. Rev. Veterinaire Can. 44, 885–897.

Smith, S., Nichols, T., 2009. Threshold-free cluster enhancement: addressing problems of smoothing, threshold dependence and localisation in cluster inference. Neuroimage 44, 83–98. https://doi.org/10.1016/j.neuroimage.2008.03.061.

Smith, S.M., 2002. Fast robust automated brain extraction. Hum. Brain Mapp. 17, 143–155. https://doi.org/10.1002/hbm.10062.

Spets, D.S., Fritch, H.A., Slotnick, S.D., 2021. Sex differences in hippocampal connectivity during spatial long-term memory. Hippocampus 31, 669–676. https://doi.org/10.1002/hipo.23319.

Stamatakis, E.A., Adapa, R.M., Absalom, A.R., Menon, D.K., 2010. Changes in resting neural connectivity during propofol sedation. PLoS ONE 5, e14224. https://doi.org/10.1371/journal.pone.0014224.

Steele, T.A., St Louis, E.K., Videnovic, A., Auger, R.R., 2021. circadian rhythm sleep-wake disorders: a contemporary review of neurobiology, treatment, and dysregulation in neurodegenerative disease. Neurother. J. Am. Soc. Exp. Neurother. 18, 53–74. https://doi.org/10.1007/s13311-021-01031-8.

Stettner, G.M., Zanella, S., Huppke, P., Gärtner, J., Hilaire, G., Dutschmann, M., 2008. Spontaneous central apneas occur in the C57BL/6J mouse strain. Respir. Physiol. Neurobiol. 160, 21–27. https://doi.org/10.1016/j.resp.2007.07.011.

Stoodley, C.J., 2012. The cerebellum and cognition: evidence from functional imaging studies. Cerebellum Lond. Engl. 11, 352–365. https://doi.org/10.1007/s12311-011-0260-7.

Sundberg, J.P., Taylor, D., Lorch, G., Miller, J., Silva, K.A., Sundberg, B.A., Roopenian, D., Sperling, L., Ong, D., King, L.E., Everts, H., 2011. Primary follicular dystrophy with scarring dermatitis in C57BL/6 mouse substrains resembles central centrifugal cicatricial alopecia in humans. Vet. Pathol. 48, 513–524. https://doi.org/10.1177/0300985810379431.

Szczesny, G., Veihelmann, A., Massberg, S., Nolte, D., Messmer, K., 2004. Long-term anaesthesia using inhalatory isoflurane in different strains of mice-the haemodynamic effects. Lab. Anim. 38, 64–69. https://doi.org/10.1258/00236770460734416.

Todd, T.P., Fournier, D.I., Bucci, D.J., 2019. Retrosplenial cortex and its role in cue-specific learning and memory. Neurosci. Biobehav. Rev. 107, 713–728. https://doi.org/10.1016/j.neubiorev.2019.04.016.

Trefler, A., Sadeghi, N., Thomas, A.G., Pierpaoli, C., Baker, C.I., Thomas, C., 2016. Impact of time-of-day on brain morphometric measures derived from T1-weighted magnetic resonance imaging. Neuroimage 133, 41–52. https://doi.org/10.1016/j.neuroimage.2016.02.034.

Vanhoutte, G., Verhoye, M., Van der Linden, A., 2006. Changing body temperature affects the T2* signal in the rat brain and reveals hypothalamic activity. Magn. Reson. Med. 55, 1006–1012. https://doi.org/10.1002/mrm.20861.

Veer, I.M., 2010. Whole brain resting-state analysis reveals decreased functional connectivity in major depression. Front. Syst. Neurosci. 4 https://doi.org/10.3389/fnsys.2010.00041.

Verweij, I.M., Onuki, Y., Van Someren, E.J.W., Van der Werf, Y.D., 2016. Sleep to the beat: a nap favours consolidation of timing. Behav. Neurosci. 130, 298–304. https://doi.org/10.1037/bne0000146.

Vivien-Roels, B., Malan, A., Rettori, M.-C., Delagrange, P., Jeanniot, J.-P., Pévet, P., 1998. Daily variations in pineal melatonin concentrations in inbred and outbred mice. J. Biol. Rhythms 13, 403–409. https://doi.org/10.1177/074873098129000228.

von Gall, C., Lewy, A., Schomerus, C., Vivien-Roels, B., Pevét, P., Korf, H.W., Stehle, J.H., 2000. Transcription factor dynamics and neuroendocrine signalling in the mouse pineal gland: a comparative analysis of melatonin-deficient C57BL mice and melatonin-proficient C3H mice. Eur. J. Neurosci. 12, 964–972. https://doi.org/10.1046/j.1460-9568.2000.00990.x.

Winkler, A.M., Ridgway, G.R., Webster, M.A., Smith, S.M., Nichols, T.E., 2014. Permutation inference for the general linear model. Neuroimage 92, 381–397. https://doi.org/10.1016/j.neuroimage.2014.01.060.

Woolrich, M.W., Behrens, T.E.J., Beckmann, C.F., Jenkinson, M., Smith, S.M., 2004. Multilevel linear modelling for FMRI group analysis using Bayesian inference. Neuroimage 21, 1732–1747. https://doi.org/10.1016/j.neuroimage.2003.12.023.

Woolrich, M.W., Ripley, B.D., Brady, M., Smith, S.M., 2001. Temporal autocorrelation in univariate linear modeling of FMRI data. Neuroimage 14, 1370–1386. https://doi.org/10.1006/nimg.2001.0931.

Worsley, K.J., 2001. Statistical analysis of activation images. In: Jezzard, P., Matthews, P. M., Smith, S.M. (Eds.), Functional Magnetic Resonance Imaging: An Introduction to Methods. Oxford University Press. https://doi.org/10.1093/acprof:oso/9780192630711.003.0014, p. 0.

Yamaguchi, Y., Suzuki, T., Mizoro, Y., Kori, H., Okada, K., Chen, Y., Fustin, J.-M., Yamazaki, F., Mizuguchi, N., Zhang, J., Dong, X., Tsujimoto, G., Okuno, Y., Doi, M., Okamura, H., 2013. Mice genetically deficient in vasopressin V1a and V1b receptors are resistant to jet lag. Science 342, 85–90. https://doi.org/10.1126/science.1238599.

Yamauchi, M., Kimura, H., Strohl, K.P., 2010. Mouse models of apnea: strain differences in apnea expression and its pharmacologic and genetic modification. Adv. Exp. Med. Biol. 669, 303–307. https://doi.org/10.1007/978-1-4419-5692-7_62.

Zerbi, V., Grandjean, J., Rudin, M., Wenderoth, N., 2015. Mapping the mouse brain with rs-fMRI: an optimized pipeline for functional network identification. Neuroimage 123, 11–21. https://doi.org/10.1016/j.neuroimage.2015.07.090.

Zhu, M., Ackerman, J.J.H., Sukstanskii, A.L., Yablonskiy, D.A., 2006. How the body controls brain temperature: the temperature shielding effect of cerebral blood flow. J. Appl. Physiol. Bethesda Md 1985 (101), 1481–1488. https://doi.org/10.1152/japplphysiol.00319.2006.